CHAPTER ONE

Leveraging the photophysical properties of rhenium(I) tricarbonyl complexes for biomedical applications

Justin J. Wilson*

Department of Chemistry and Chemical Biology, Cornell University, Ithaca, NY, United States
*Corresponding author: e-mail address: jjw275@cornell.edu

Contents

Abstract

Rhenium(I) tricarbonyl ($Re(CO)_3$) complexes have been extensively studied for their photochemical and catalytic properties. In recent years, it has been recognized that complexes of this class can also be applied favorably for various diagnostic and therapeutic biomedical applications. In particular, their rich photophysical properties make them amenable for use as optical imaging agents, as well as photoactivated or photodynamic therapeutic agents. Despite the recent rapid expansion of research in this area over the last 5 years, this chapter presents only a narrow, detailed focus on contributions to this field by the Wilson Laboratory in the Department of Chemistry and Chemical Biology at Cornell University. This chapter begins with a brief description of the photophysical properties of $Re(CO)_3$ complexes that make them valuable for biomedical applications. Subsequently, a discussion on the earliest and most prominent examples of how these complexes were used for imaging is presented. The rest of the chapter focuses specifically on anticancer $Re(CO)_3$ complexes developed by the Wilson Lab. These examples highlight mechanistic studies that show how these compounds are distinct from

Advances in Inorganic Chemistry, Volume 80
ISSN 0898-8838
https://doi.org/10.1016/bs.adioch.2022.04.005

conventional platinum anticancer agents and how the ligand choice can affect biological activities. Furthermore, the use of the rich photophysical properties of these anticancer agents for both imaging and photoactivation is discussed.

Abbreviations

ABC	ATP-binding cassette
ATF4	activating transcription factor 4
bisim	bidentate diimine ligand
bpy	2,2′-bipyridine
CHOP	C/EBP homologous protein
DAPTA	3,7-diacetyl-1,3,7-triaza-5-phosphabicyclo[3.3.1]nonane
DFT	density functional theory
DMSO	dimethylsulfoxide
eIF2α	eukaryotic translation initiation factor 2 subunit 1
ER	endoplasmic reticulum
FPR	formyl peptide receptor
GSH	glutathione
H&E	hematoxylin and eosin
HPLC	high-performance liquid chromatography
Hsp90	heat shock protein 90
ic	internal conversion
IC_{50}	50% growth inhibitory concentration
isc	intersystem crossing
LF	ligand field
MDR	multidrug resistance
MLCT	metal-to-ligand charge transfer
MTT	3-(4,5-dimethylthiazol-2-yl)-2,5-diphenyltetrazolium bromide
neo	neocuproine
PACT	photoactivated chemotherapy
PDT	photodynamic therapy
Pgp	P-glycoprotein
PTA	1,3,5-triaza-7-phosphaadamantane
ROS	reactive oxygen species
RT-PCR	reverse transcriptase-polymerase chain reaction
SAR	structure-activity relationship
THP	tris(hydroxymethyl)phosphine
UV	ultraviolet
XRF	X-ray fluorescence

1. Introduction

The unique properties of transition metal coordination and organometallic complexes, relative to organic molecules, have facilitated their use in a wide range of applications. This aspect is apparent in the field

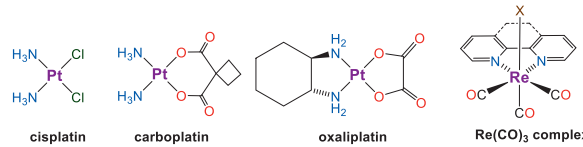

Fig. 1 Structures of the clinically used Pt anticancer drugs cisplatin, carboplatin, and oxaliplatin and the general structure of a $Re(CO)_3$ complex.

of medicine, where metal-based compounds have experienced clinical success as both diagnostic and therapeutic agents.[1–5] With respect to therapeutic applications, the platinum (Pt) compounds cisplatin, carboplatin, and oxaliplatin are among the most widely used and well known metal-containing drugs (Fig. 1).[6] The success of these chemotherapeutic agents has motivated extensive research to develop new Pt-based drug candidates.[7–9] Despite these significant efforts, the advancement of new Pt compounds to clinical trials and beyond has been met with challenges, including dose-limiting toxic side effects and acquired resistance.[10,11]

Driven to overcome the limitations of conventional Pt-based drugs, inorganic chemists have investigated complexes of other metal ions for their biomedical applications. Most notably, researchers in this field have recognized the potential use of transition metal photochemistry for this application.[12–15] In this regard, polypyridyl complexes of the precious metals ruthenium (Ru), osmium (Os), iridium (Ir), and rhenium (Re) have been the subject of most of these studies.[16–22] These complexes exhibit rich photophysical properties that have enabled their use as photoluminescent imaging agents as well as photoactivated and photodynamic therapeutic agents. Among these metal complexes, Re(I) tricarbonyl ($Re(CO)_3$) compounds (Fig. 1) have undergone an expansive growth in their investigation for biomedical applications within the last several years.[23–26] Researchers have found that this class of compounds has a number of favorable properties for both imaging and therapeutic applications. With respect to therapeutic applications, early studies have shown that $Re(CO)_3$ complexes typically exhibit ligand substitution rates that are comparable to the clinically used Pt anticancer agents.[27–29] As such, these complexes have the potential to bind to and interact with intracellular targets on a biologically relevant timescale.[28,30–34] Furthermore, when coupled with appropriate supporting ligands, the $Re(CO)_3$ core possesses valuable photoluminescent properties that can be leveraged for fluorescence microscopy imaging.[35–37] In addition to optical imaging, the intense CO stretching modes of these complexes have also been used in a wide range of vibrational microscopy techniques for visualizing their cellular uptake and intracellular distribution.[38,39]

Lastly, the ability to synthesize analogous tricarbonyl complexes of technetium (Tc), the lighter congener of Re, has enabled the use of its radioisotope ^{99m}Tc for nuclear imaging applications.[40–43] Collectively, both the therapeutic potential and diverse imaging modalities accessible to $Re(CO)_3$ complexes have led to a surge in their biomedical applications.

In this Chapter, we will discuss recent developments from our laboratory in the use of $Re(CO)_3$ complexes in biology. A broad overview of the properties of these complexes followed by some of their applications in cellular imaging, anticancer therapy, and phototoxicity studies will be presented. Given the significant expansion of this field, the scope of this chapter will be focused on work carried out specifically by our lab with several key examples from other research teams when relevant.

2. Properties and applications of $Re(CO)_3$ complexes

The $Re(CO)_3$ core is a robust organometallic fragment that has been incorporated into a number of different molecules. $Re(CO)_3$ complexes bearing aromatic diimine ligands, first reported in 1941,[44] possess a number of interesting photochemical properties that make them useful for different applications. For example, the low-energy empty π^* orbitals of these ligands render metal-to-ligand charge transfer (MLCT) excited states to be accessible in the near ultraviolet (UV) and visible region of the spectrum.[45,46] Coupled with efficient intersystem crossing afforded by the large spin-orbit coupling of the heavy Re center, these compounds are often photoluminescent through the triplet MLCT (^{3}MLCT) excited state. The rich photochemistry of these complexes has been the subject of intense investigation since the 1960s and has been critical to developing a number of fundamental principles in the field of inorganic photochemistry.[47–51] In addition, the catalytic properties of these complexes have been heavily investigated. In particular, $Re(CO)_3$ complexes are efficient photocatalysts and electrocatalysts for the reduction of CO_2 and H^+.[52,53] A large body of work has probed the mechanisms of these transformations as catalyzed by $Re(CO)_3$ complexes, and the effects of ligand modifications on their catalytic efficiencies.[54–58]

The potential biological applications of this photochemistry are dictated by the fate of the rapidly generated ^{3}MLCT excited state (Fig. 2). If this state is energetically far from low-lying ligand field (LF) states, radiative decay becomes the dominant pathway for relaxation, leading to compounds that are suitable for optical imaging applications. Depending on the supporting ligands, however, the ^{3}LF state can be sufficiently lowered in energy, such

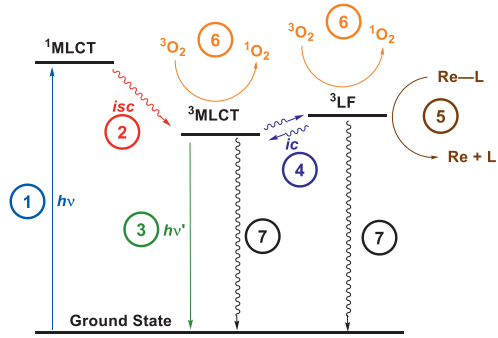

Fig. 2 Simplified Jablonski diagram demonstrating the potential fates of the ^{3}MLCT excited state of diimine $Re(CO)_3$ complexes that depend on the nature of the supporting ligands: (1) Diimine $Re(CO)_3$ complexes absorb light to populate the ^{1}MLCT state. (2) Intersystem crossing (isc) occurs rapidly to the ^{3}MLCT state. Once in the ^{3}MLCT state, (3) these complexes can relax to the ground state by emitting a photon, a process that would make them valuable as optical imaging agents. Alternatively, (4) internal conversion (ic) to thermally accessible ^{3}LF states may be possible. From the ^{3}LF state, (5) photosubstitution can occur readily, favoring the use of $Re(CO)_3$ complexes as PACT agents. Similarly, in either the ^{3}MLCT and ^{3}LF states, (6) energy transfer to ground state $^3O_2$ can take place, leading to the generation of cytotoxic $^1O_2$. $Re(CO)_3$ complexes that undergo this pathway can be leveraged as PDT agents. Lastly, (7) non-radiative relaxation to the ground state may be the dominant process. $Re(CO)_3$ complexes of this type may still be biologically active in the absence of light and useful for anticancer applications.

that it is thermally accessible from the ^{3}MLCT excited state. In these cases, excitation of the $Re(CO)_3$ complexes can lead to efficient photosubstitution reactions via population of the dissociative ^{3}LF excited states.[59] Complexes of this type have the potential to act as photoactivated chemotherapeutic (PACT) agents, or compounds that trigger light-induced cancer cell death without generating singlet oxygen ($^1O_2$). The use of $Re(CO)_3$ complexes as photodynamic therapeutic (PDT) agents, compounds that generate cytotoxic $^1O_2$, is also possible, as both the ^{3}MLCT and ^{3}LF excited states typically have sufficient energy to convert ground state triplet oxygen ($^3O_2$) to $^1O_2$.[22] The efficiency of this process is dictated by the energy difference between the Re and O_2 excited states, the respective lifetimes of the Re excited states, and the concentration of O_2. Compounds with effective $^1O_2$-sensitization capabilities can be leveraged as PDT agents, which elicit cancer cell death via the generation of this potent reactive oxygen species (ROS). Lastly, if non-radiative decay via other pathways occurs efficiently, the ^{3}MLCT returns to the ground state. Compounds for which this pathway is the dominant process may still be biologically active in the absence of light. Importantly, the relative energies and accessibilities of

non-radiative decay pathways can be largely controlled by the nature of supporting ligands on these complexes. As such, $Re(CO)_3$ complexes provide a robust and diverse framework to capitalize on different photobiological applications by varying the types of ligands used.

3. $Re(CO)_3$ complexes as photoluminescent imaging agents

The earliest studies involving $Re(CO)_3$ in biological environments sought to leverage their rich photophysical properties for imaging applications. In a landmark investigation in 2004, a $Re(CO)_3$ complex bearing a tridentate bis(quinolyl) amine ligand was conjugated to a peptide, fMLF(SAACQ)G, that binds to the formyl peptide receptor (FPR). This receptor is overexpressed on neutrophils and has been used in nuclear medicine as a means of tracking white blood cells. This complex fMLF [(SAACQ-$Re(CO)_3)^+$]G (Fig. 3) was successfully used for fluorescence imaging and flow cytometry of human leukocytes.[60] Furthermore, its corresponding isostructural ^{99m}Tc complex was also prepared as a nuclear imaging partner. Shortly after this initial report, a second study on the optical imaging applications of $Re(CO)_3$ complexes of the formula $[Re(bisim)L(CO)_3]^+$, where bisim is a bidentate diimine and L is a monodentate pyridine ligand, were reported in 2007.[61] In this work, both the bisim ligand and the monodentate pyridine analogues were systematically modified to investigate their effects on the photophysical properties and intracellular distribution of the resulting complexes. These compounds were imaged in a parasitic flagellate *Spironucleus vortens*. The researchers found that ligand modifications not only altered the emission energies and quantum yields of the complexes, but also affected their toxicity and susceptibility to photobleaching in the parasite. The complex bearing a sulfonated phenanthroline and hydroxymethyl pyridine ligand was found to possess optimal cell uptake

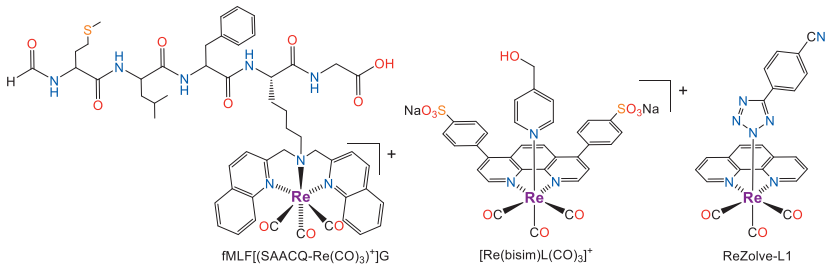

Fig. 3 Structures of several of the earliest used and most prominent $Re(CO)_3$ biological imaging agents.

with low toxicity, suggesting its value as an optical imaging agent (Fig. 3). Together, these two initial studies highlighted the promise and viability of $Re(CO)_3$ complexes bearing tridentate and a mixture of bidentate and monodentate ligands. Many subsequent efforts have been undertaken to explore these two classes of $Re(CO)_3$ complexes for optical imaging applications. One of the most significant outcomes of these efforts has been the development and commercialization of the $Re(CO)_3$ tetrazolato complex with the trade name ReZolve-L1™ (Fig. 3).[62] This neutral $Re(CO)_3$ complex selectively stains lipid droplets, enabling their imaging by two-photon fluorescence microscopy and Fourier transform infrared microspectroscopy in human adipocytes and adipose cells from *Drosophila*.[63–65] Importantly, this compound was applied as a tool to study the distinct lipid profiles of human prostate cancer cell lines (Fig. 4).[66] Furthermore, an analogue of

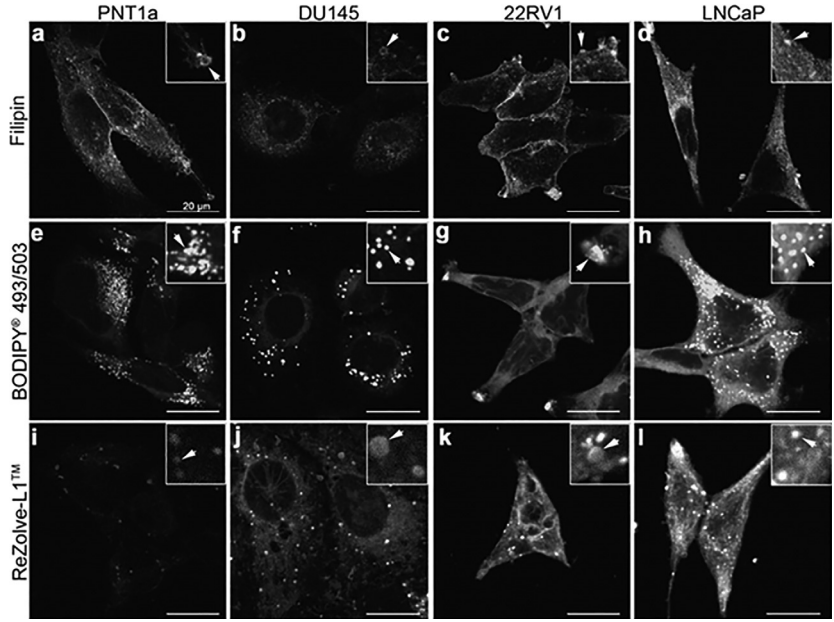

Fig. 4 Fluorescence microscopy images of the non-malignant prostate cell line PNT1a, and the prostate cancer cell lines DU145, 22RV1, and LNCaP treated with either Filipin III (a stain for free cholesterol), BODIPY® 493/503 (a stain for cholesteryl esters and triacylglycerides), or ReZolve-L1™. Cells in panels (A–H) were fixed with 4% paraformaldehyde, and those in panels (I–K) were imaged live. The scale bars are 20 µm. These images show how ReZolve-L1™ is able to identify distinct lipid droplet profiles within the prostate cancer cells lines. *Reproduced with permission from Sorvina, A.; Bader, C.A.; Caporale, C.; Carter, E.A.; Johnson, I.R.D.; Parkinson-Lawrence, E.J.; Simpson, P.V.; Wright, P.J.; Stagni, S.; Lay, P.A.; Massi, M.; Brooks, D.A.; Plush, S.E.* Oncotarget ***2018,*** *9, 35541–35552. Copyright 2018 Impact Journals, LLC.*

ReZolve-L1™ bearing a pyridyl tetrazolato ligand was found to selectively localize to the endoplasmic reticulum (ER),[67] thus demonstrating how the imaging applications of these $Re(CO)_3$ complexes can be modified with appropriate ligand choices. Given that our laboratory has focused mostly on the therapeutic applications of $Re(CO)_3$, this topic will not be discussed in greater detail and readers are referred to other comprehensive review articles on their optical imaging applications.[14,35,36,39,68–70]

4. Simple diimine $Re(CO)_3$ complexes exhibit anticancer activity

Based on the favorable photoluminescent properties and ligand substitution kinetics of $Re(CO)_3$ complexes, our lab was interested in the possibility of using these complexes as theranostic anticancer agents.[71] This interest was further bolstered by prior studies that demonstrated some $Re(CO)_3$ complexes to possess cytotoxic and antitumor activities in the absence of light irradiation.[72,73] In our initial efforts towards discovering new $Re(CO)_3$ anticancer agents, we prepared a small library of these complexes bearing different diimine ligands based on both 2,2′-bipyridine (bpy) and 1,10-phenathroline (phen) to carry out a simple in vitro screening of their anticancer activities.[74] To improve aqueous solubility and biocompatibility, we used these compounds in their cationic aquated forms, where the axial ligand is a neutral aqua ligand. Our screening of this small compound library revealed them to inhibit cancer cell growth within the micromolar concentration range. Notably, one compound identified, Neo-Re or $[Re(CO)_3(neo)(OH_2)]^+$ where neo = neocuproine (Fig. 5), was more potent than the reference metallodrug cisplatin in HeLa cells.

The potent anticancer properties of this complex in HeLa cells prompted us to carry out additional biological studies to understand its mechanism

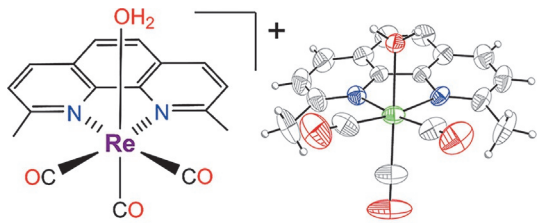

$[Re(CO)_3(neo)(OH_2)]^+$
Neo-Re

Fig. 5 Structure of Neo-Re, a cytotoxic $Re(CO)_3$ anticancer agent.

of action. The cross-resistance of this compound with cisplatin was assessed by testing its in vitro anticancer activity in both wild-type A2780 and cisplatin-resistant A2780CP70 ovarian cancer cells, as well as wild-type KB-3-1 and cisplatin-resistant KBCP20 cervical cancer cells. Although Neo-Re was less potent in the wild-type cell lines compared to cisplatin, it was more active against the cisplatin-resistant variants and exhibited no differential activities between the two cell line pairs. As such, these data clearly showed that Neo-Re could circumvent the platinum-resistance mechanisms within these cell lines. This latter result highlights the fact that these compounds act via a distinct mechanism of action.

To further study its mechanism of action, we carried out a series of biological studies to probe for canonical modes of cell death. Intriguingly, a combination of flow cytometric studies, western blots, and cytotoxicity assays in the presence of different cell death pathway inhibitors failed to paint a clear picture of a canonical form of cell death that Neo-Re could be inducing in cancer cells. In terms of other phenotypic responses of cancer cells treated with Neo-Re, the formation of enlarged endosomes and lysosomes within the cytoplasm occurred (Fig. 6). The apparent perturbation of these organelles is consistent with our cellular uptake studies that showed it to enter cells via endocytosis. Although a specific molecular target has not yet been conclusively identified, a COMPARE analysis[75] of data obtained from an NCI-60 screen[76] showed that the spectrum of activity of this compound correlated highly with other compounds that are known inhibitors of the chaperone heat shock protein 90 (Hsp90).[77] A large subset of the known Hsp90 inhibitors interact with this protein via covalent interactions with key cysteine residues.[78] Similarly, the labile aqua ligand present in Neo-Re provides an opportunity for this compound to form covalent interactions with potential protein targets. Our work and those of others has shown that these $Re(CO)_3$ have a strong affinity for sulfur donors like cysteine and glutathione (GSH),[74,79–81] suggesting that their biological activities may arise in part from these types of interactions. This latter concept was demonstrated with a similar library of compounds that was shown to inhibit a key protease responsible for the virulence of the SARS-CoV-2 virus by forming covalent adducts with a cysteine residue.[81]

Based on the promising in vitro anticancer activity of Neo-Re, the in vivo antitumor properties of this compound were assessed in mice bearing an ovarian cancer patient-derived xenograft.[82] These mice were injected twice weekly via tail vein injection with either 10, 20, or 40 mg/kg of Neo-Re. These doses were able to slow tumor growth over a period of

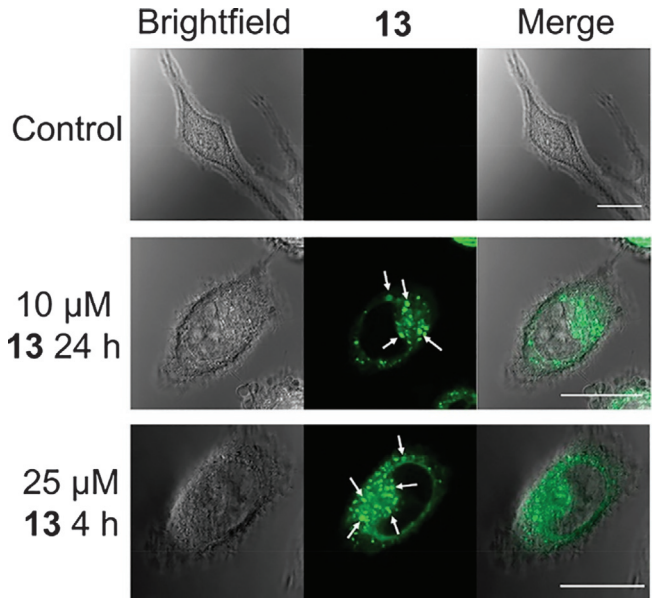

Fig. 6 Confocal fluorescence microscope images of HeLa cells in the absence or presence of Neo-Re (**13** in this figure). The photoluminescence of this compound was imaged directly, enabling the detection of vacuolization of the cytosol as indicated by the white arrows. Scale bars are 20 μm. *Reproduced with permission from Knopf, K. M.; Murphy, B. L.; MacMillan, S. N.; Baskin, J. M.; Barr, M. P.; Boros, E.; Wilson, J. J.* J. Am. Chem. Soc. ***2017,*** 139*, 14302–14314. Copyright 2017 American Chemical Society.*

30 days. Notably, no differences in tumor growth were observed between the three administered doses, suggesting that higher doses beyond 10 mg/kg afford no additional beneficial biological effects. The body weight of all three mice cohorts did not decrease over the duration of this experiment, indicating that Neo-Re is well tolerated. This latter aspect was verified via histological studies, which showed no morphological abnormalities in sensitive organs like the kidneys and liver. Overall, these in vivo studies underscore the potential for compounds like Neo-Re as anticancer agents.

5. Pyridylimine $Re(CO)_3$ complexes

Based on the promising anticancer activities of the simple bpy and phen complexes discussed above, we sought alternative bidentate ligands that could also confer $Re(CO)_3$ complexes with cytotoxic activity. In this regard, pyridylimine ligands, which can be synthesized via a simple condensation reaction between an amine and a picolinaldehyde, provide a versatile

platform by which the properties of these compounds could be systematically modified. Indeed, pioneering work by Ziegler and coworkers in this area has shown that this condensation reaction can be a straightforward means of attaching biologically relevant groups, like peptides, amino acids and fluorophores, to the $Re(CO)_3$ core.[83–86] Furthermore, pyridylimine ligands have been previously studied for their use in a wide range of different metal-based anticancer agents.[87] In particular, the facile assembly of these ligands from various picolinaldehydes and amines was used to generate a combinatorial library of different Ru arene complexes within a 96-well plate, which was then screened directly for anticancer activity.[88,89] Importantly, this work was able to identify novel Ru-based anticancer agents that induce ER stress.[90–92]

Motivated by these prior studies, we sought a combinatorial synthesis of $Re(CO)_3$ pyridylimine complexes for anticancer activity screening.[93] Like the prior studies involving Ru arene complexes, we varied both the picolinaldehyde and amine components along the columns and rows of a 96-well plate. In each well, $Re(CO)_5Cl$ was added to act as the template for the condensation reaction and to form complexes of the general formula $[Re(CO)_3(pyridylimine)Cl]$ directly in each well. Upon mixing of these three components in each well in dimethyl sulfoxide (DMSO), the reaction required microwave irradiation to proceed (Fig. 7). Each well was then assayed by high-performance liquid chromatography (HPLC) to assess the formation and purities of the pyridylimine $Re(CO)_3$ complexes. The majority of wells displayed >80% conversion to the pyridylimine-containing product, demonstrating the success of this approach.

Following the generation of this compound library, 10 μM concentrations of these samples were transferred to a 96-well plate containing either HeLa, A2780, or A2780CP70 cancer cells to assess their effects on cell viability via the 3-(4,5-dimethylthiazol-2-yl)-2,5-diphenyltetrazolium bromide (MTT) assay. Of the 96 compounds prepared, only three were significantly cytotoxic (Fig. 7). These three compounds share the common dimethylamino functional group on the pyridylimine ligand, suggesting that this feature is critical for anticancer activity within this class of compounds. Following this initial screen, they were independently synthesized and isolated at >95% purity. The assessment of the in vitro anticancer activity of these purified compounds revealed them to also possess potent cytotoxic activity in cancer cell lines, verifying that the intact Re complex, rather than impurities or ligand fragments, is responsible for the biological properties observed from our combinatorial screening efforts.

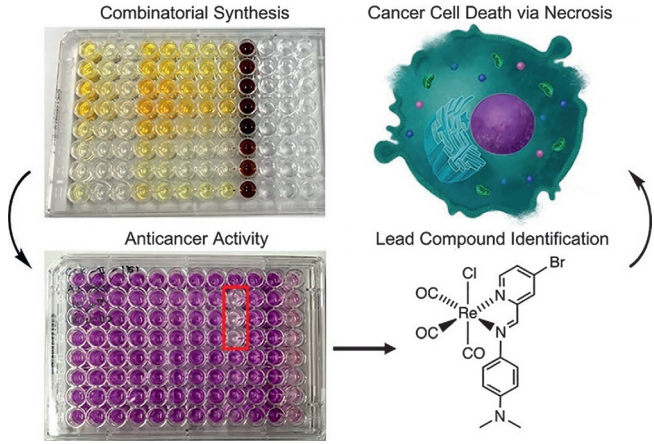

Fig. 7 Combinatorial synthetic strategy for identifying anticancer-active $Re(CO)_3$ pyridylimine complexes. (Top left) A mixture of different amines and picolinaldehydes with $Re(CO)_5Cl$ were subjected to microwave irradiation to generate a library of $[Re(CO)_3(pyridylimine)Cl]$ complexes. (Bottom left) These complexes were then transferred directly to a 96-well plate containing cancer cells and screened for cytotoxic activity with the MTT assay. (Bottom right) From these screening efforts, three potent $[Re(pyridylimine)Cl(CO)_3]$ complexes were identified. The most effective compound, Re-9D (shown), was synthesized and purified independently. (Top right) The biological mechanism of action of Re-9D was studied, revealing it to induce cell death via necrosis. *Reproduced with permission from Konkankit, C.C.; Vaughn, B.A.; MacMillan, S.N.; Boros, E.; Wilson, J.* J. Inorg. Chem. ***2019,*** 58*, 3895–3909. Copyright 2019 American Chemical Society.*

Mechanistically, these pyridylimine $Re(CO)_3$ complexes are distinct from both cisplatin and Neo-Re. They are equally potent in both wild-type and cisplatin-resistant ovarian cancer cells, reflecting a lack of cross resistance with cisplatin. Both brightfield and fluorescence microscopy was used to further probe the mechanism of action of the most potent compound in this class Re-9D (Fig. 7), revealing distinct differences from Neo-Re as well. Within several hours of compound treatment, the outer membrane of cancer cells becomes permeabilized and cytoplasmic expulsion occurs. This rapid outer membrane permeabilization was also detected with the fluorescent dye propidium iodide, which can only enter cells with compromised membranes (Fig. 8). The membrane permeabilization and cytoplasmic expulsion induced by Re-9D suggest that it causes canonical necrotic cell death in cancer cells, in contrast to Neo-Re.

Building upon these studies, we targeted alternative pyridylimine complexes that may possess potent cytotoxic activities. We rationalized that

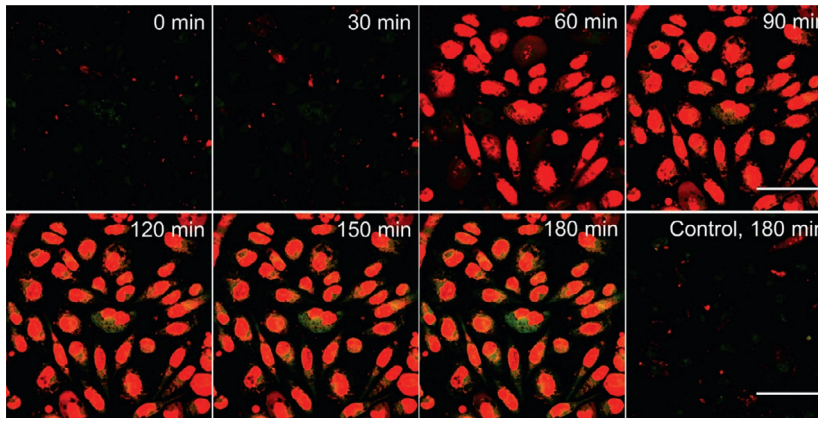

Fig. 8 A2780CP70 cells treated with 60 μM Re-9D and propidium iodide imaged by confocal fluorescence microscopy over 180 min. The influx and nuclear staining of propidium iodide is caused by the necrotic rupture of the cell membranes upon exposure to Re-9D. Scale bars are 100 μm. *Reproduced from Konkankit, C.C.; Vaughn, B.A.; MacMillan, S.N.; Boros, E.; Wilson, J.* J. Inorg. Chem. ***2019,*** 58, *3895–3909. Copyright 2019, American Chemical Society.*

increasing the compound lipophilicity would enhance the cellular uptake and cytotoxic activities of this class of compounds. This phenomenon has previously been exploited to develop highly active platinum-based drug candidates[94–98] and has also been explored in the context of different $Re(CO)_3$ complexes primarily for imaging applications.[86,99,100] Using this modular condensation chemistry, picolinaldehyde and amines with different alkyl chain lengths, ranging from 2 to 12 carbons, were attached to the $Re(CO)_3$ core to make a series of complexes with varying lipophilicities (Fig. 9).[101] The water-octanol partition coefficients (log *P* values) of these complexes ranged from 1.59 to 2.95, demonstrating that these values could be tuned with the length of the alkyl chain. Unexpectedly, the 50% growth inhibitory concentration (IC_{50}) values of all six of these complexes in HeLa cells were identical after a 48-h incubation period (Fig. 10A). However, the use of different incubation times with these compounds enabled us to detect significant variations on their effects on cell viability. In particular, compounds with longer alkyl chains reduced cell viability more effectively over shorter incubation time periods, but these differential cytotoxic effects were not apparent over longer time frames (Fig. 10B). This result highlights the significance of testing the effect of time in biological studies and how physiochemical property differences, like lipophilicity, may only be apparent at early time points. Several other studies have also

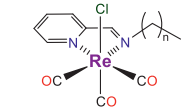

n = 1 (**Re-C2**), n = 2 (**Re-C3**)
n = 3 (**Re-C4**), n = 4 (**Re-C5**)
n = 5 (**Re-C5**), n = 11 (**Re-C12**)

Fig. 9 Structures of $Re(CO)_3$ pyridylimine complexes bearing different alkyl chain substituents.

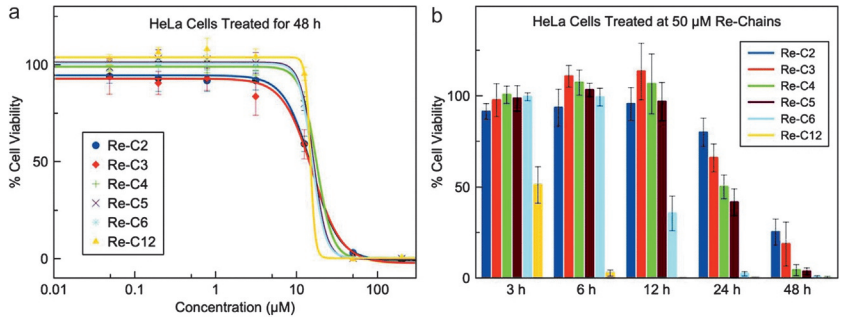

Fig. 10 (A) Dose-response curves of HeLa cells treated with the $Re(CO)_3$ pyridylimine alkyl chain complexes, named in Fig. 9, for a 48-h incubation period. No significant differences in cytotoxic activity over this time point were observed. (B) Single-dose 50 μM-treatment of HeLa cells with the $Re(CO)_3$ pyridylimine alkyl chain complexes for variable incubation times. Notably, compounds with longer alkyl chains induce their cytotoxic effects more rapidly. *Reproduced with permission from Konkankit, C.C.; Vaughn, B.A.; Huang, Z.; Boros, E.; Wilson, J.* J. Dalton Trans. ***2020,*** *49, 16062–16066. Copyright 2020 Royal Society of Chemistry.*

begun to investigate the kinetics of cellular uptake of metal-based drug candidates as an important parameter in determining their viability and use in different therapeutic and diagnostic applications.[102,103]

6. Isonitrile-containing $Re(CO)_3$ complexes

Isonitriles are π-acceptor ligands that share many common features with CO. Although they can generate metal complexes with similar chemical properties as CO, a potential advantage of isonitriles is that they can be modified by altering the substituents on the nitrogen atom. This amenability to structural diversity has led to the use of these ligands for different biomedical applications. Most notably, the clinically used perfusion imaging agent, Cardiolite®, is a homoleptic ^{99m}Tc isonitrile complex.[104] Furthermore, $Re(CO)_3$ complexes bearing these ligands have rich

photophysical properties that could be leveraged for imaging applications.[105,106] Based on these favorable properties, we began to explore the use of isonitriles as ligands for new cytotoxic $Re(CO)_3$ complexes.

In our initial screening studies, we identified a tricarbonyl rhenium isonitrile polpyridyl (TRIP) complex of the formula $[Re(CO)_3(neo)(isc)]^+$, where isc = *p*-tolylisonitrile, that exhibits potent in vitro anticancer activity (Fig. 11).[107] In A2780 ovarian cancer cells, the cytotoxicity of this compound exceeds that of cisplatin, suggesting that it could be a valuable therapeutic agent. Furthermore, like the other $Re(CO)_3$ compounds described above, TRIP is not cross-resistant with cisplatin, a property that is reflected by its equitoxic effects in both wild-type A2780 and cisplatin-resistant A2780CP70 ovarian cancer cell lines. A key difference between TRIP and the other $Re(CO)_3$ complexes discussed above is that it contains no labile ligands, a property that was verified with X-ray fluorescence (XRF) microscopy. For these XRF studies, an analogue of TRIP containing an iodine (I) on the axial isonitrile ligand (I-TRIP) was used.[108] HeLa cells treated with I-TRIP were imaged by XRF microscopy, and these imaging studies showed that Re and I co-localized with one another, indicating that the isonitrile ligand does not dissociate from the Re coordination sphere intracellularly (Fig. 12). These results are in contrast to the $Re(CO)_3$ aqua and chlorido complexes described above, where the axial ligands are known to undergo facile ligand substitution reactions with biological nucleophiles,

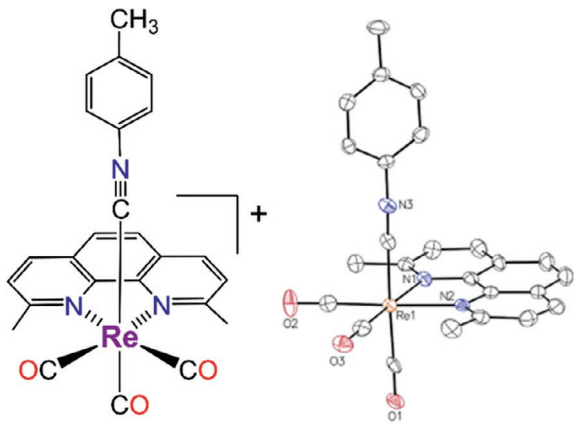

Fig. 11 Structure of the isonitrile-$Re(CO)_3$ complex TRIP.

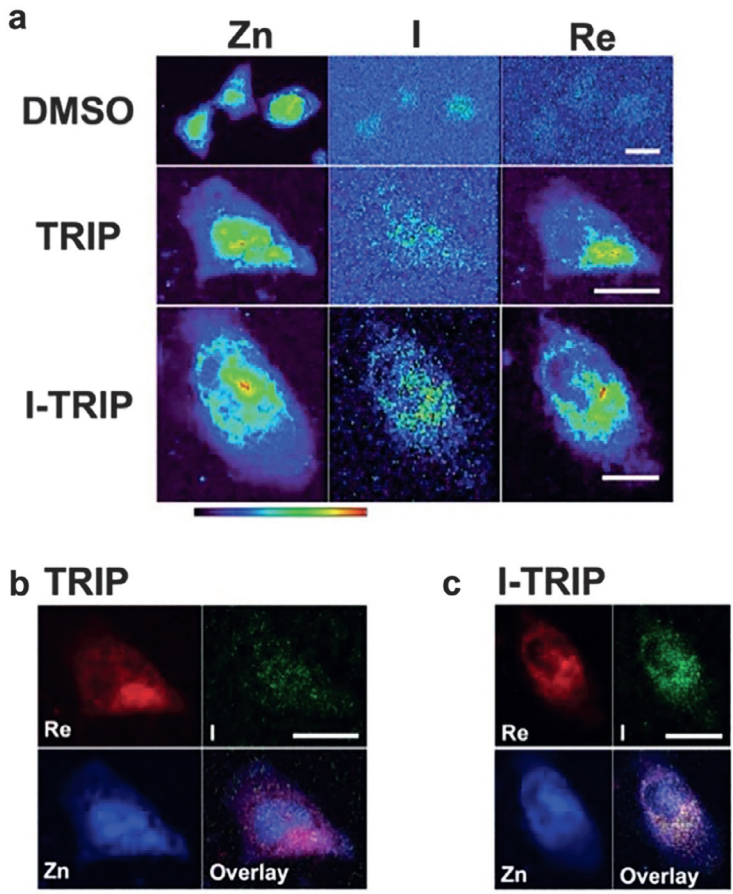

Fig. 12 (A) XRF maps displaying the elemental distribution of Zn, I, and Re within HeLa cells treated with either DMSO (0.06% v/v), 2 mM TRIP, or 3 mM I-TRIP. Correlation analysis on the co-localization of Re, I, and Zn distribution maps for cells treated with (B) TRIP and (C) I-TRIP. The scale bar is 20 μm. *Reproduced with permission from Konkankit, C.C.; Lovett, J.; Harris, H.H.; Wilson, J.* J. Chem. Commun. ***2020,*** 56*, 6515–6518. Copyright 2020 Royal Society of Chemistry.*

but are similar to those obtained for iodine-labeled analogues of the tetrazolate-bearing $Re(CO)_3$ imaging agent ReZolve™, for which the axial tetrazolate ligand also remained bound in cells.[109] Collectively, these studies show how $Re(CO)_3$ complexes can be altered to afford either covalent inhibitors or intact structural inhibitors.[110]

Given the different chemical reactivity of TRIP, its biological mechanism of action was of particular interest. Fluorescence microscopy studies

revealed this compound to induce mitochondrial fission 30 min post-treatment, which was then related to the ability of this compound to trigger apoptotic and autophagic cell death. Moreover, because mitochondrial fission and autophagy are frequently related to ER stress,[111] we investigated the role of this phenomenon in the mechanism of TRIP. Western blots of cell lysates from cancer cells treated with TRIP revealed this compound to induce phosphorylation of the transcription factor eIF2α. This transcription factor is a regulator of the unfolded protein response (UPR), a mechanism of cellular response to ER stress.[112] We further showed that the downstream consequences of eIF2α phosphorylation, namely the inhibition of translation and the upregulation of pro-apoptotic stress response factors ATF4 and CHOP,[113] also occurred. Collectively, these data support the fact that TRIP is capable of causing ER stress in cancer cells, which in turn leads to translation inhibition and cell death. To investigate the mechanisms by which this compound induces ER stress, we used the dye thioflavin T, which elicits a fluorescent response in the presence of protein aggregates, to show that TRIP increases the misfolded protein burden in cancer cells within a short 30 min time period. Based on these data, a mechanistic hypothesis for TRIP was formulated and is summarized in Fig. 13.

As noted in Section 1, a key limitation of the Pt-based drugs arises from the ability of cancer cells to develop resistance to them.[114] Although we showed that TRIP is not cross-resistant with cisplatin, we considered the possibility that ovarian cancer cells may be able to develop alternative resistance mechanisms to circumvent the biological properties of this $Re(CO)_3$ complex. In addition to highlighting potential deficiencies of TRIP, the identification of resistance pathways is valuable in gaining a deeper mechanistic insight on this compound, as drug resistance mechanisms have previously been correlated to specific biological targets for novel therapeutic agents.[115,116] The treatment of A2780 ovarian cancer cells with TRIP at doses below its IC_{50} value for over a year afforded a resistant cell line A2780TR, which required a ninefold higher concentration of TRIP to elicit an equivalent cytotoxic effect compared to the wild-type A2780 cell line.[117] Although the Pt-based drugs cisplatin, carboplatin, and oxaliplatin were not cross-resistant in this cell line, the organic drug taxol exhibited a remarkable 180-fold decrease in potency in the TRIP-resistant cell line.

The significant cross-resistance between TRIP and taxol indicated that taxol-resistance mechanisms were also likely a key factor in the observed TRIP resistance mechanisms. In this context, one of the most predominant

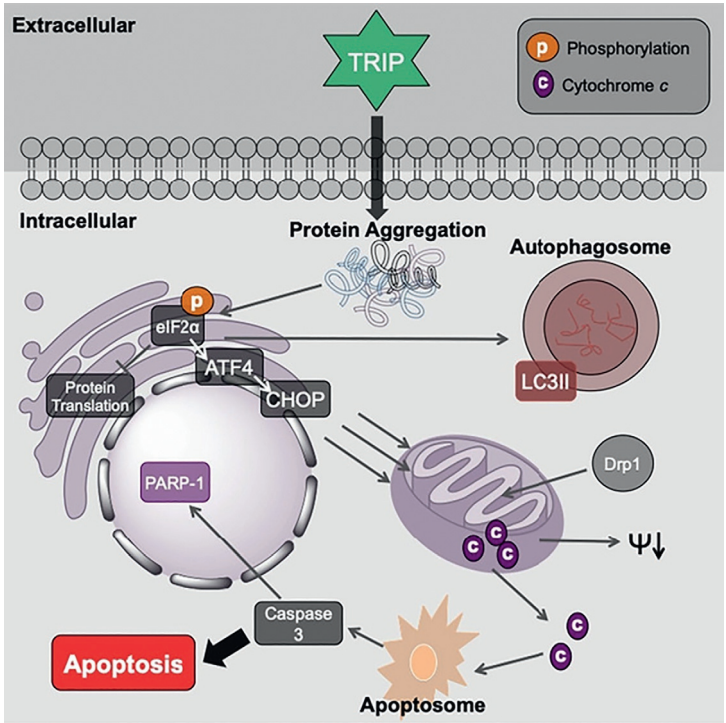

Fig. 13 Summary of the proposed mechanism of anticancer activity of TRIP. *Reproduced with permission from King, A.P.; Marker, S.C.; Swanda, R.V.; Woods, J.J.; Qian, S.-B.; Wilson, J.* J. Chem. A Eur. J. ***2019,*** 25, *9206–9210. Copyright 2019 Wiley-VCH.*

mechanisms of resistance to taxol is the upregulation of the ATP-binding cassette (ABC) transporter P-glycoprotein (Pgp).[118] The upregulation of Pgp, which effluxes a wide range of different organic drugs from cells, is a common component of the multidrug resistance (MDR) pathway that is prevalent among drug-treated cancer cells and tumors.[119] Consistent with this hypothesis, we observed that TRIP-resistance could be reversed by the Pgp inhibitor verapamil and that cellular uptake of TRIP, as measured by both fluorescence microscopy and inductively coupled plasma optical emission spectroscopy, was significantly diminished in the TRIP-resistant cell line. Lastly, Pgp-encoding mRNA levels in the A2780 and A2780TR cell lines were determined with reverse transcriptase-polymerase chain reaction (RT-PCR). These studies revealed that the resistant cell line contains 800 times more Pgp-encoding mRNA than the wild-type cell line. Thus, these data demonstrate that Pgp is an important efflux transporter for TRIP that mediates cancer cell resistance to this compound. Although Pgp has long

been implicated in cancer resistance to organic drugs, these studies support the role of this transporter in mediating inorganic and organometallic complex drug resistance mechanisms. For example, in addition to our work with TRIP, earlier studies have shown that the ^{99m}Tc imaging agent Cardiolite®,[120] the Pt-based drug oxaliplatin,[121] the anti-arthritic gold drug auronafin,[122] the anti-metastatic Ru drug candidate KP1019,[123] and cyclometalated Ru and Os ER stress-inducers[124] are also substrates of Pgp. Thus, the role of Pgp in xenobiotic efflux processes may extend beyond conventional organic drugs and be more significant for the detoxification of metal-containing chemical compounds.

Based on the promising anticancer activity of TRIP and its novel mechanism of protein aggregation and ER stress induction, we next sought to find improved analogues and develop structure-activity relationships (SARs) for this compound class. A small library of 11 $Re(CO)_3$ complexes containing different diimine and isonitrile ligands was synthesized (Fig. 14). These ligands were chosen to modify both the lipophilic and electronic properties of the complexes and to assess their importance in mediating their cytotoxic activities in HeLa cells. Although no strong dependence on the lipophilicity was observed, several correlations with the electron-donating strengths of the ligands were observed. For example, both the CO and isonitrile CN vibrational stretching frequencies correlated with

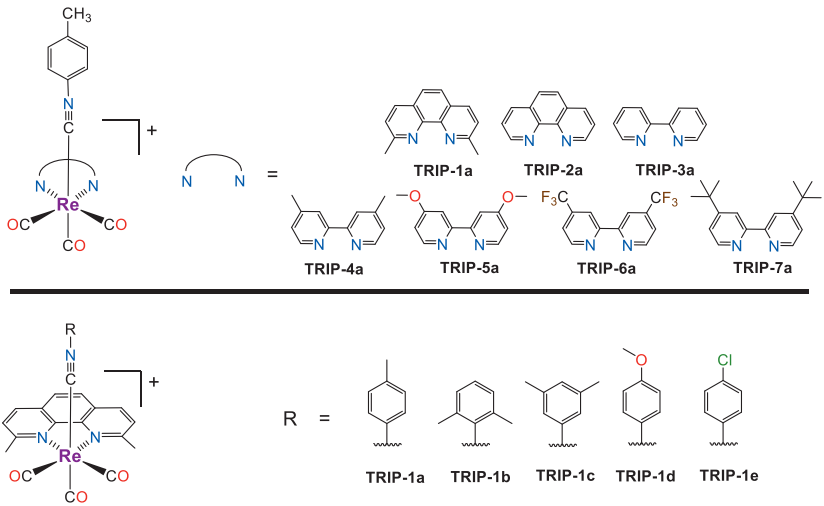

Fig. 14 Structures and naming scheme of the 11 different TRIP analogues investigated for the SARs in Ref. 125. TRIP-1a is the same compound named TRIP, shown in Fig. 11.

the cytotoxic activities of these complexes. Specifically, lower energy stretching frequencies, a property that will arise in more electron-rich metal centers, were indicative of more potent compounds. In addition to probing the cytotoxic properties of this compound library, we also investigated their mechanisms of action. Importantly, we found that this compound library triggered the same phenotypic responses in cancer cells as TRIP (Fig. 15). Specifically, these compounds upregulated CHOP, caused

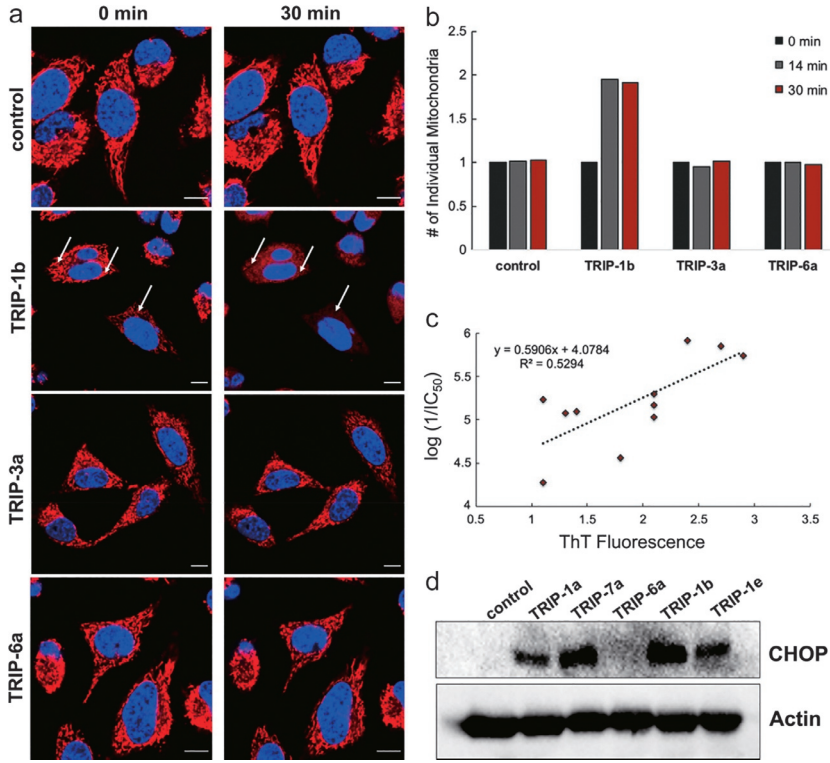

Fig. 15 Biological mechanistic studies and SARs of the TRIP analogs, which are named as shown in Fig. 14. (A) HeLa cells treated with 10 μM of the indicated TRIP analog stained with MitoTracker red and Hoechst. Arrows indicate signs of mitochondrial fission after a 30-min treatment period. Scale bars are 10 μm. (B) Quantification of the number of mitochondria resulting from fission after treatment with 10 μM of the indicated TRIP analog. (C) Plot of cytotoxic activity, log(1/IC_{50}), of the TRIP analogs vs intracellular thioflavin T fluorescence in HeLa cells, showing a correlation between these two properties. (D) CHOP expression levels shown by western blot in HeLa cells treated with the indicated TRIP analog for 24 h. *Reproduced with permission from Marker, S.C.; King, A.P.; Granja, S.; Vaughn, B.; Woods, J.J.; Boros, E.; Wilson, J.* J. Inorg. Chem. ***2020,*** *59, 10285–10303. Copyright 2020 American Chemical Society.*

mitochondrial fission, and induced intracellular protein aggregation. Furthermore, the extent of protein aggregation caused by these compounds was correlated directly with their cytotoxic activities, confirming that this phenotypic response is a critical component of their mechanism of action. The observation that all of these compounds within the library exhibited the same biological mechanism of action is important, especially in the context of developing rational SAR. An interesting problem in the field of medicinal inorganic chemistry is that often times simple ligand modifications can dramatically alter the mechanism of action.[90,126–128] These significant mechanistic changes can make it difficult to improve biological activity and pharmacokinetic properties as the resulting biological effects may be different.

Following the promising in vitro studies with TRIP and its analogues, the in vivo antitumor properties and biodistribution of this compound were assessed. For the biodistribution studies, a ^{99m}Tc analogue of TRIP, called TTIP, was prepared to determine its suitability as a diagnostic partner for this therapeutic agent. Both compounds overall showed very similar biodistribution patterns with pronounced accumulation in the kidneys and heart. The kidney uptake can be explained by the renal clearance of these compounds, whereas the heart accumulation is consistent with the lipophilic cationic nature of these compounds that favors accumulation in the mitochondria-rich cardiac cells and the high expression levels of Pgp within this tissue. Following these biodistribution studies, the in vivo antitumor activity of TRIP (TRIP-1a) was assessed in mice bearing ovarian cancer A2780 xenografts. The mice were treated with TRIP twice weekly via tail vein injection. As shown in Fig. 16, the administered dose of 20 mg/kg was able to slow tumor growth in a statistically significant manner, resulting in prolonged survival of the mice. In addition, only minimal changes in body weight were observed, and histological analysis with hematoxylin and eosin (H&E) staining revealed no detectable morphological changes in organ composition. Thus, TRIP appears to be well-tolerated in vivo. In addition to our mouse study of Neo-Re, [82] described above in Section 4, there have only been a limited number of investigations of this type using $Re(CO)_3$ complexes, but they collectively reveal the promising in vivo antitumor potential of this class of compounds.[129–134] Altogether, our in-depth studies of TRIP and its analogues as promising anticancer agents highlight the increasingly recognized importance of metal complexes as novel ER stress-inducers and protein translation inhibitors.[135,136]

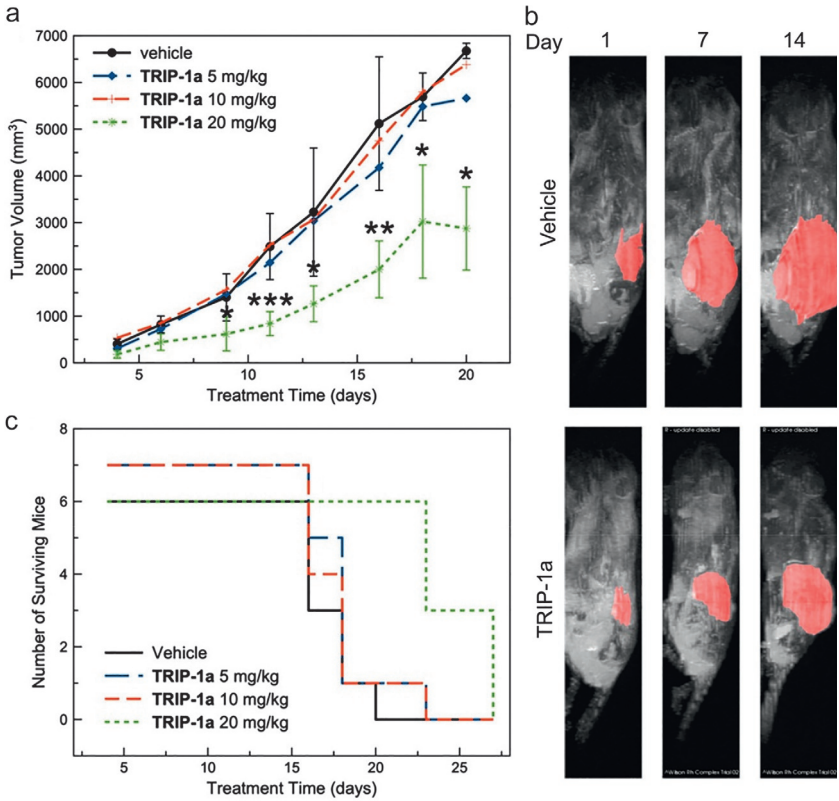

Fig. 16 In vivo antitumor efficacy of TRIP (TRIP-1a) in mice bearing A2780 ovarian cancer xenografts. (A) Tumor volume of mice treated with the indicated doses of TRIP (* = $P < 0.05$, ** = $P < 0.01$, *** = $P < 0.005$). (B) Magnetic resonance images of mice treated with either the vehicle control or TRIP. The tumor xenograft is marked in red. (C) Kaplan-Meier survival plot of mice treated with TRIP over the duration of the study. *Reproduced with permission from Marker, S.C.; King, A.P.; Granja, S.; Vaughn, B.; Woods, J.J.; Boros, E.; Wilson, J.* J. Inorg. Chem. ***2020,*** 59, *10285–10303. Copyright 2020 American Chemical Society.*

7. Photoactivation of $Re(CO)_3$ anticancer agents

In addition to providing valuable applications in imaging, the rich photophysical properties of the late 2nd and 3rd row transition metal complexes have also been harnessed for developing photoactivated anticancer agents. The majority of complexes of this type are based on Ru and Ir[16,137] with substantially fewer examples for Re.[21] Despite the paucity of photoactivated Re-based anticancer agents reported to date, several early

studies highlighted the value of these complexes for this application. It has been demonstrated that $Re(CO)_3$ complexes bearing suitable diimine or quinolylamine ligands generate $^1O_2$ upon photoirradiation, which can trigger photoactivated cell death in cancer cells.[138–141] Notably, by changing the nature of the ligands, photoactivation with biocompatible red light could be achieved.[142]

Although the generation of $^1O_2$ is a highly effective means of inducing cell death via PDT, this type of photoactivation requires high concentrations of oxygen, which is often depleted in the hypoxic tumor microenvironment. By contrast, the concept of PACT uses ligand photosubstitution processes to generate cytotoxic compounds. PACT has been developed extensively in the context of Ru polypyridyl complexes for which the control of ligand substitution reactions by light has been thoroughly studied.[143–145] Compared to Ru, the photolabile ^{3}LF states of $Re(CO)_3$ complexes are higher in energy, making photosubstitution much rarer for this compound class. In 2000, the group of Ishitani discovered that $Re(CO)_3$ complexes of the general formula $[Re(CO)_3(NN)(PR_3)]^+$, where NN is a diimine ligand, are photolabile, ejecting the CO trans to the phosphine upon 365-nm light irradiation.[146] Although the ^{3}LF excited state is still higher in energy than the initially populated ^{3}MLCT state, it is thermally accessible at room temperature.[147] The photochemistry of this class of compounds was leveraged to design light-activated CO-releasing molecules as tools to study the biological properties of this small gasotransmitter.[148–150]

In studying this photochemistry, we recognized that the aqua-$Re(CO)_2$ byproduct $[Re(CO)_2(OH_2)(NN)(PR_3)]^+$ generated upon light irradiation may also have biological activity, given its structural similarity to the cytotoxic Neo-Re compound discussed above in Section 3. To investigate this hypothesis, we synthesized a series of compounds with different diimine and phosphine ligands (Fig. 17).[151] The three phosphine ligands tris(hydroxymethyl)phosphine (THP), 1,3,5-triaza-7-phosphaadamantane (PTA), and 3,7-diacetyl-1,3,7-triaza-5-phosphabicyclo[3.3.1]nonane (DAPTA) were chosen for this study because they are known to confer their coordination compounds with good water solubility.[152–154] These compounds were administered to HeLa cells at a single 200 μM dose, and their cytotoxicities were evaluated in either the absence or presence of 365-nm light irradiation for 30 min with the MTT assay. With the exception of those bearing the PTA phosphine, these compounds are non-toxic in the dark, but can elicit effective cell-killing properties upon exposure to light (Fig. 18). The lack of phototoxicity of the PTA complexes could be

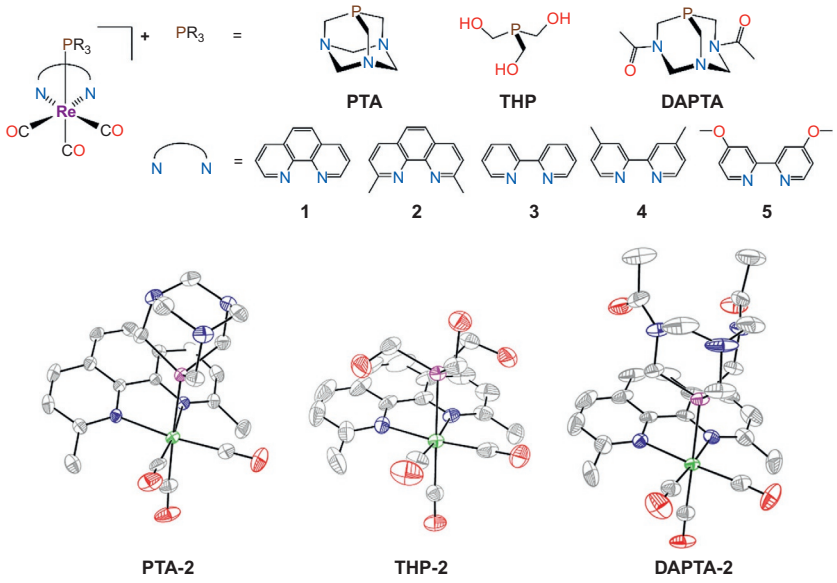

Fig. 17 Structures of the photoactive $Re(CO)_3$ anticancer complexes investigated in Ref. 151.

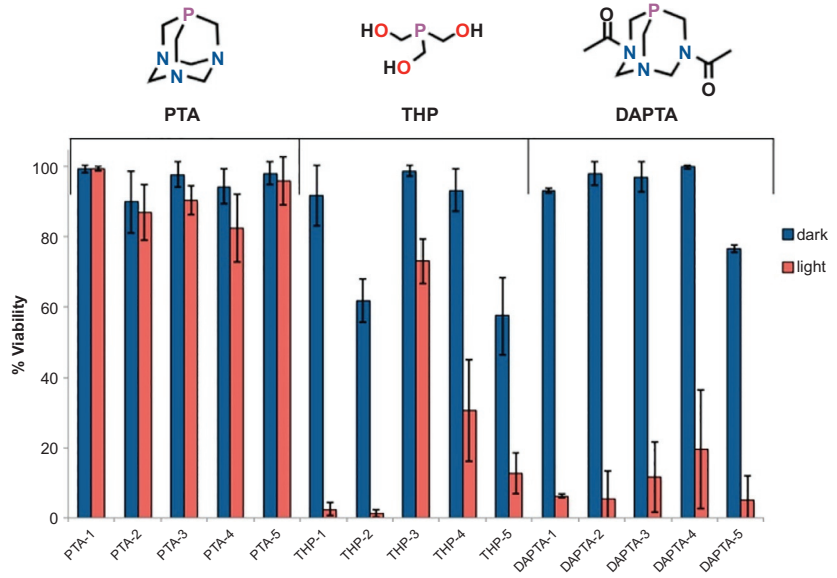

Fig. 18 Cell viability of HeLa cells treated with 200 μM of the indicated compound, named as shown in Fig. 17. After treatment, cells were either kept in the dark or irradiated with 365-nm light for 30 min at a photon flux of 2.4×10^{-10} einsteins/s. *Reproduced with permission from Marker, S.C.; MacMillan, S.N.; Zipfel, W.R.; Li, Z.; Ford, P.C.; Wilson, J.* J. Inorg. Chem. ***2018,*** *57, 1311–1331. Copyright 2018 American Chemical Society.*

a consequence of photoinduced electron transfer quenching of their excited states by the nitrogen lone pairs on this ligand. Complexes with the DAPTA phosphine show the most promising phototoxic effects. Thus, proper tuning of the ligand coordination sphere to modulate excited state energies can lead to effective photoactivated Re-based anticancer agents, as verified by recent computational studies on this subject.[155]

The means by which these compounds induce their light-activated anticancer activities was further assessed with the most potent phototoxic compound, $[Re(CO)_3(phen)(DAPTA)]^+$ (DAPTA-1). Its photoproduct, the aqua complex $[Re(CO)_2(H_2O)(phen)(DAPTA)]^+$ (DAPTA-1A) was synthesized and isolated independently, and its cytotoxic activity in HeLa cells was measured. The IC_{50} value of this compound was found to be approximately 40 μM, roughly an order of magnitude less potent than DAPTA-1 upon photoirradiation. These results indicated that the phototoxic effects of DAPTA-1 cannot be attributed solely to the Re photoproducts. It was further determined that these compounds can sensitize the formation of $^1O_2$ with quantum yields up to 70%, thus suggesting another mode by which these compounds can kill cells in the presence of light. Lastly, the cytotoxic and anticancer properties of CO have been well documented,[156] and may also be a contributing factor for these complexes. These compounds are therefore most likely acting in a multi-pronged manner with respect to their abilities to induce phototoxic effects.

We have also explored other approaches to leverage the photochemical properties of $Re(CO)_3$ complexes to design photoactivated drug candidates. Towards these efforts and motivated by other heterometallic multinuclear $Re(CO)_3$ complexes[157] and Pt(IV) complexes with photoactive ligands,[158–160] we have developed multimetallic complexes comprising one Pt(IV) and two $Re(CO)_3$ centers.[161] The Pt(IV) core can act as a prodrug for the conventional Pt(II)-based anticancer agents upon its reduction,[9] whereas the $Re(CO)_3$ centers were chosen for both their ER stress-inducing and photochemical properties. We hypothesized that these conjugates would elicit a dual mechanism of cytotoxicity, with the Pt fragment forming covalent DNA crosslinks and the $Re(CO)_3$ compounds causing ER stress. Conjugates containing Pt(IV) analogues of cisplatin and oxaliplatin, CisPtRe and OxaliPtRe, were synthesized and compared to the mononuclear $Re(CO)_3$ analogue, TRIP-suc (Fig. 19). Upon treatment of CisPtRe or OxaliPtRe with 20 equiv. of the biological reducing agent GSH over 24 h, partial reduction of the Pt(IV) center with concomitant release of the axial ligand TRIP-suc is observed. Consistent with previous comparative studies on the reduction of Pt(IV) analogs of oxaliplatin and

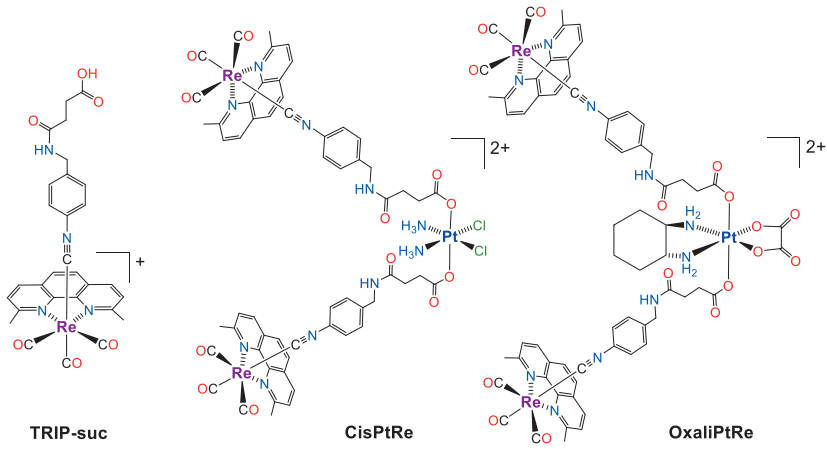

Fig. 19 Structures of the Pt(IV)-Re(I) conjugates investigated in Ref. 161.

cisplatin,[162] the extent of reduction of OxaliPtRe (<5%) was significantly smaller than that of CisPtRe (35%) over the same time period. In addition to being activated by chemical reduction, these compounds can undergo a photochemical reaction. Irradiation with 365-nm light triggers the photoreduction of the Pt(IV) center, releasing both the Pt(II) analogues and TRIP-suc. Importantly, the photoreduction occurs on a much faster timescale than chemical reduction by GSH, suggesting that these compounds could be useful as photoactivated drug candidates. The mechanism of photoreduction of these compounds was investigated by density functional theory (DFT) (Fig. 20). In this case, light irradiation of the TRIP-suc axial ligands induces a transition from the d(π) orbitals to the ligand π^* orbitals, yielding a $Re(CO)_3$-based MLCT excited state. The Pt(IV) d(σ^*) orbitals energetically reside between the Re d(π) and ligand π^* orbitals. Therefore, once populated the ligand π^* orbitals of the Re center can transfer the electron to the Pt(IV) d(σ^*) orbitals, leading to photoreduction and ligand dissociation from the Pt(IV) center. Based on this photochemical activation process, we assessed the cytotoxicity of these compounds both in the dark and upon light irradiation to determine their viabilities as light-activated drug candidates. Only mild increases in cytotoxicity (2–3 fold) were observed upon light irradiation. The low phototoxicity indices suggested that other factors, such as cell uptake and intracellular localization, may also play an important role in mediating their cytotoxic activities. These compounds show that $Re(CO)_3$ centers can play a role that is distinct from $^1O_2$-generation and photoinduced ligand substitution

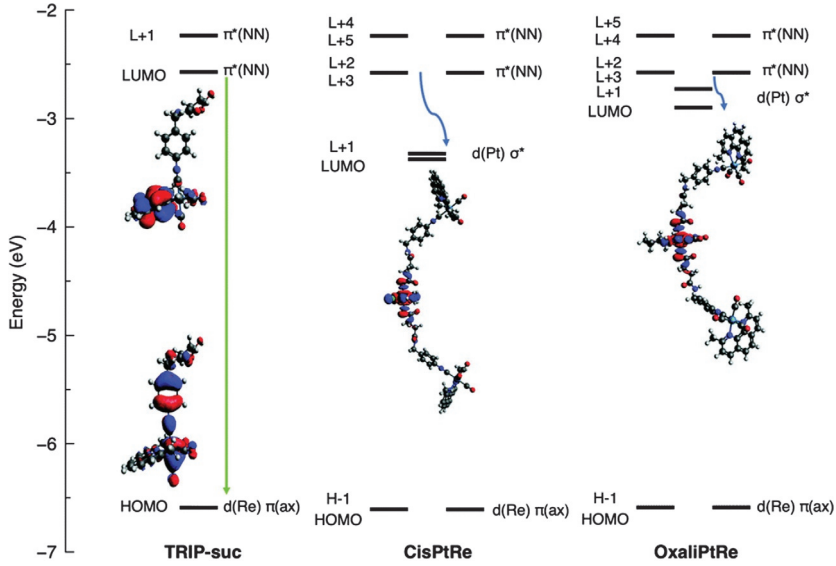

Fig. 20 Frontier Kohn-Sham molecular orbitals, as calculated by DFT, for TRIP-suc, CisPtRe, and OxaliPtRe. The green arrow represents an emissive transition from the ^{3}MLCT state. The blue arrows represent photoinduced electron transfer non-radiative decay pathways through the intermediary unoccupied Pt σ* d orbitals. *Reproduced with permission from Huang, Z.; King, A.P.; Lovett, J.; Lai, B.; Woods, J.J.; Harris, H.H.; Wilson, J.* J. Chem. Commun. ***2021,*** *57, 11189–11192. Copyright 2021 Royal Society of Chemistry.*

pathways discussed prior. Specifically, CisPtRe and OxaliPtRe demonstrate that the $Re(CO)_3$ core can act as a photoreductant, providing a novel means of photoactivation.

8. Conclusions and future outlook

The biological applications of $Re(CO)_3$ complexes are rapidly expanding as researchers recognize how the novel photophysical properties of these systems can be leveraged in unique manners. Although many researchers have explored these complexes, the examples described above highlight specific case studies and contributions from our own lab. Through these efforts, we have demonstrated several important concepts and points of interest that may motivate continued investigations in this area. Specifically, the rich spectroscopic properties of this compound class have proven to be valuable for understanding their mechanisms of action. For example, the fluorescence microscopy studies of Neo-Re in cells

revealed its ability to perturb lysosomal and endosomal function. In addition, the modular coordination chemistry of $Re(CO)_3$ complexes has enabled a diverse range of easily accessible compounds that can be obtained via straightforward ligand substitution or metal ion-templated condensation reactions. This principle was demonstrated in our combinatorial synthesis of pyridylimine $Re(CO)_3$ complexes. Lastly, the photochemistry of this compound class can be leveraged for a range of photobiological properties. Compounds that sensitize $^1O_2$, undergo photosubstitution, and act as photoreductants can be accessed with appropriate ligand modifications, and these features can be used for triggering photoinduced cell death. In conjunction with our work and the great contributions by numerous other research groups over the last 5 years, $Re(CO)_3$ complexes have proven to be valuable tools for therapy and diagnosis.

Acknowledgments

My former and current students Dr. A. Paden King, Dr. Sierra C. Marker, Dr. Chilaluck C. Konkankit, Mr. Kevin M. Knopf, and Mr. Tracky Huang are thanked for their invaluable contributions to this project and research area. Early research in our lab in this area was supported by the Department of Defense Ovarian Cancer Research Program under award no. W81XWH-17-1-0097.

References

1. Guo, Z.; Sadler, P. J. *Angew. Chem. Int. Ed.* **1999**, *38*, 1512–1531.
2. Chellan, P.; Sadler, P. J. *Phil. Trans. R. Soc. A* **2015**, *373*, 20140182.
3. Anthony, E. J.; Bolitho, E. M.; Bridgewater, H. E.; Carter, O. W. L.; Donnelly, J. M.; Imberti, C.; Lant, E. C.; Lermyte, F.; Needham, R. J.; Palau, M.; Sadler, P. J.; Shi, H.; Wang, F.-X.; Zhang, W.-Y.; Zhang, Z. *Chem. Sci.* **2020**, *11*, 12888–12917.
4. Imberti, C.; Sadler, P. J. *Adv. Inorg. Chem.* **2020**, *75*, 3–56.
5. Farrell, N. P. *Adv. Inorg. Chem.* **2020**, *75*, 57–86.
6. Johnstone, T. C.; Suntharalingam, K.; Lippard, S. J. *Chem. Rev.* **2016**, *116*, 3436–3486.
7. Wang, Z.; Deng, Z.; Zhu, G. *Dalton Trans.* **2019**, *48*, 2536–2544.
8. Khoury, A.; Deo, K. M.; Aldrich-Wright, J. R. *J. Inorg. Biochem.* **2020**, *207*, 111070.
9. Xu, Z.; Wang, Z.; Deng, Z.; Zhu, G. *Coord. Chem. Rev.* **2021**, *442*, 213991.
10. Peng, K.; Liang, B.-B.; Liu, W.; Mao, Z.-W. *Coord. Chem. Rev.* **2021**, *449*, 214210.
11. Ivanova, S. *Pharmacia* **2022**, *69*, e78813.
12. Monro, S.; Colón, K. L.; Yin, H.; Roque, J., III; Konda, P.; Gujar, S.; Thummel, R. P.; Lilge, L.; Cameron, C. G.; McFarland, S. A. *Chem. Rev.* **2019**, *119*, 797–828.
13. Imberti, C.; Zhang, P.; Huang, H.; Sadler, P. J. *Angew. Chem. Int. Ed.* **2020**, *59*, 61–73.
14. Xu, G.-X.; Mak, E. C.-L.; Lo, K. K.-W. *Inorg. Chem. Front.* **2021**, *8*, 4553–4579.
15. Karges, J. *Angew. Chem. Int. Ed.* **2022**, *61*, e202112236.
16. Mari, C.; Gasser, G. *Chimia* **2015**, *69*, 176–181.
17. Mari, C.; Pierroz, V.; Ferrari, S.; Gasser, G. *Chem. Sci.* **2015**, *6*, 2660–2686.
18. Huang, H.; Banerjee, S.; Sadler, P. J. *ChemBioChem* **2018**, *19*, 1574–1589.
19. Huang, T.; Yu, Q.; Liu, S.; Huang, W.; Zhao, Q. *Dalton Trans.* **2018**, *47*, 7628–7633.

20. Zhang, P.; Huang, H. *Dalton Trans.* **2018**, *47*, 14841–14854.
21. Liew, H. S.; Mai, C.-W.; Zulkefeli, M.; Madheswaran, T.; Kiew, L. V.; Delsuc, N.; Low, M. L. *Molecules* **2020**, *25*, 4176.
22. Wolcan, E. *Inorg. Chim. Acta* **2020**, *509*, 119650.
23. Leonidova, A.; Gasser, G. *ACS Chem. Biol.* **2014**, *9*, 2180–2193.
24. Bauer, E. B.; Haase, A. A.; Reich, R. M.; Crans, D. C.; Kühn, F. E. *Coord. Chem. Rev.* **2019**, *393*, 79–117.
25. Collery, P.; Desmaele, D.; Veena, V. *Curr. Pharm. Des.* **2019**, *25*, 3306–3322.
26. Schindler, K.; Zobi, F. *Molecules* **2022**, *27*, 539.
27. Salignac, B.; Grundler, P. V.; Cayemittes, S.; Frey, U.; Scopelliti, R.; Merbach, A. E.; Hedinger, R.; Hegetschweiler, K.; Alberto, R.; Prinz, U.; Raabe, G.; Kölle, U.; Hall, S. *Inorg. Chem.* **2003**, *42*, 3516–3526.
28. Zobi, F.; Spingler, B.; Fox, T.; Alberto, R. *Inorg. Chem.* **2003**, *42*, 2818–2820.
29. Schutte-Smith, M.; Marker, S. C.; Wilson, J. J.; Visser, H. G. *Inorg. Chem.* **2020**, *59*, 15888–15897.
30. Oriskovich, T. A.; White, P. S.; Thorp, H. H. *Inorg. Chem.* **1995**, *34*, 1629–1631.
31. Zobi, F.; Spingler, B.; Alberto, R. *ChemBioChem* **2005**, *6*, 1397–1405.
32. Binkley, S. L.; Leeper, T. C.; Rowlett, R. S.; Herrick, R. S.; Ziegler, C. J. *Metallomics* **2011**, *3*, 909–916.
33. Zobi, F.; Spingler, B. *Inorg. Chem.* **2012**, *51*, 1210–1212.
34. Santoro, G.; Blacque, O.; Zobi, F. *Metallomics* **2012**, *4*, 253–259.
35. Lo, K. K.-W.; Zhang, K. Y.; Li, S. P.-Y. *Eur. J. Inorg. Chem.* **2011**, 3551–3568.
36. Lee, L. C.-C.; Leung, K.-K.; Lo, K. K.-W. *Dalton Trans.* **2017**, *46*, 16357–16380.
37. Schindler, K.; Zobi, F. *Chimia* **2021**, *75*, 837–844.
38. Clède, S.; Policar, C. *Chem. A Eur. J.* **2015**, *21*, 942–958.
39. Hostachy, S.; Policar, C.; Delsuc, N. *Coord. Chem. Rev.* **2017**, *351*, 172–188.
40. Alberto, R.; Ortner, K.; Wheatley, N.; Schibli, R.; Schubiger, A. P. *J. Am. Chem. Soc.* **2001**, *123*, 3135–3136.
41. Pitchumony, T. S.; Banevicius, L.; Janzen, N.; Zubieta, J.; Valliant, J. F. *Inorg. Chem.* **2013**, *52*, 13521–13528.
42. Yazdani, A.; Janzen, N.; Banevicius, L.; Czorny, S.; Valliant, J. F. *Inorg. Chem.* **2015**, *54*, 1728–1736.
43. Dilworth, J. R.; Parrott, S. J. *Chem. Soc. Rev.* **1998**, *27*, 43–55.
44. Hieber, W.; Fuchs, H. *Z. Anorg. Allg. Chem.* **1941**, *248*, 269–275.
45. Vogler, A.; Kunkely, H. *Coord. Chem. Rev.* **2000**, *200–202*, 991–1008.
46. Kumar, A.; Sun, S.-S.; Lees, A. J. *Top. Organomet. Chem.* **2010**, *29*, 1–35.
47. Wrighton, M.; Morse, D. L. *J. Am. Chem. Soc.* **1974**, *96*, 998–1003.
48. Wrighton, M. S.; Morse, D. L.; Pdungsap, L. *J. Am. Chem. Soc.* **1975**, *97*, 2073–2079.
49. Giordano, P. J.; Wrighton, M. S. *J. Am. Chem. Soc.* **1979**, *101*, 2888–2897.
50. Fredericks, S. M.; Luong, J. C.; Wrighton, M. S. *J. Am. Chem. Soc.* **1979**, *101*, 7415–7417.
51. Summers, D. P.; Luong, J. C.; Wrighton, M. S. *J. Am. Chem. Soc.* **1981**, *103*, 5238–5241.
52. Grice, K. A.; Kubiak, C. P. *Adv. Inorg. Chem.* **2014**, *66*, 163–188.
53. Zarkadoulas, A.; Koutsouri, E.; Kefalidi, C.; Mitsopoulou, C. A. *Coord. Chem. Rev.* **2015**, *304–305*, 55–72.
54. Kurz, P.; Probst, B.; Spingler, B.; Alberto, R. *Eur. J. Inorg. Chem.* **2006**, 2966–2974.
55. Chabolla, S. A.; Dellamary, E. A.; Machan, C. W.; Tezcan, F. A.; Kubiak, C. P. *Inorg. Chim. Acta* **2014**, *422*, 109–113.
56. Vollmer, M. V.; Machan, C. W.; Clark, M. L.; Antholine, W. E.; Agarwal, J.; Schaefer, H. F., III; Kubiak, C. P.; Walensky, J. R. *Organometallics* **2015**, *34*, 3–12.
57. Clark, M. L.; Cheung, P. L.; Lessio, M.; Carter, E. A.; Kubiak, C. P. *ACS Catal.* **2018**, *8*, 2021–2029.

58. Shirley, H.; Sexton, T. M.; Liyanage, N. P.; Palmer, C. Z.; McNamara, L. E.; Hammer, N. I.; Tschumper, G. S.; Delcamp, J. H. *Eur. J. Inorg. Chem.* **2020**, 1844–1851.
59. Sato, S.; Ishitani, O. *Coord. Chem. Rev.* **2015**, *282–283*, 50–59.
60. Stephenson, K. A.; Banerjee, S. R.; Besanger, T.; Sogbein, O. O.; Levadala, M. K.; McFarlane, N.; Lemon, J. A.; Boreham, D. R.; Maresca, K. P.; Brennan, J. D.; Babich, J. W.; Zubieta, J.; Valliant, J. F. *J. Am. Chem. Soc.* **2004**, *126*, 8598–8599.
61. Amoroso, A. J.; Coogan, M. P.; Dunne, J. E.; Fernández-Moreira, V.; Hess, J. B.; Hayes, A. J.; Lloyd, D.; Millet, C.; Pope, S. J. A.; Williams, C. *Chem. Commun.* **2007**, 3066–3068.
62. Gillam, T. A.; Sweetman, M. J.; Bader, C. A.; Morrison, J. L.; Hayball, J. D.; Brooks, D. A.; Plush, S. E. *Coord. Chem. Rev.* **2018**, *375*, 234–255.
63. Bader, C. A.; Brooks, R. D.; Ng, Y. S.; Sorvina, A.; Werrett, M. V.; Wright, P. J.; Anwer, A. G.; Brooks, D. A.; Stagni, S.; Muzzioli, S.; Silberstein, M.; Skelton, B. W.; Goldys, E. M.; Plush, S. E.; Shandala, T.; Massi, M. *RSC Adv.* **2014**, *4*, 16345–16351.
64. Bader, C. A.; Carter, E. A.; Safitri, A.; Simpson, P. V.; Wright, P.; Stagni, S.; Massi, M.; Lay, P. A.; Brooks, D. A.; Plush, S. E. *Mol. BioSyst.* **2016**, *12*, 2064–2068.
65. Bader, C. A.; Shandala, T.; Carter, E. A.; Ivask, A.; Guinan, T.; Hickey, S. M.; Werrett, M. V.; Wright, P. J.; Simpson, P. V.; Stagni, S.; Voelcker, N. H.; Lay, P. A.; Massi, M.; Plush, S. E.; Brooks, D. A. *PLoS One* **2016**, *11*, e0161557.
66. Sorvina, A.; Bader, C. A.; Caporale, C.; Carter, E. A.; Johnson, I. R. D.; Parkinson-Lawrence, E. J.; Simpson, P. V.; Wright, P. J.; Stagni, S.; Lay, P. A.; Massi, M.; Brooks, D. A.; Plush, S. E. *Oncotarget* **2018**, *9*, 35541–35552.
67. Bader, C. A.; Sorvina, A.; Simpson, P. V.; Wright, P. J.; Stagni, S.; Plush, S. E.; Massi, M.; Brooks, D. A. *FEBS Lett.* **2016**, *590*, 3051–3060.
68. Balasingham, R. G.; Coogan, M. P.; Thorp-Greenwood, F. L. *Dalton Trans.* **2011**, *40*, 11663–11674.
69. Lo, K. K.-W. *Acc. Chem. Res.* **2015**, *48*, 2985–2995.
70. Yip, A. M.-H.; Lo, K. K.-W. *Coord. Chem. Rev.* **2018**, *361*, 138–163.
71. Tan, C.-P.; Zhong, Y.-M.; Ji, L.-N.; Mao, Z.-W. *Chem. Sci.* **2021**, *12*, 2357–2367.
72. Orsa, D. K.; Haynes, G. K.; Pramanik, S. K.; Iwunze, M. O.; Greco, G. E.; Ho, D. M.; Krause, J. A.; Hill, D. A.; Williams, R. J.; Mandal, S. K. *Inorg. Chem. Commun.* **2008**, *11*, 1054–1056.
73. Orsa, D. K.; Nettles, C. R.; Pramanik, S. K.; Iwunze, M. O.; Greco, G. E.; Krause, J. A.; Mandal, S. K. Cytotoxic effects of rhenium (I) carbonyl complexes on prostate cancer cell lines. In *Handbook of Prostate Cancer Cell Research*; Nova Science Publishers, Inc.: Hauppauge, NY, 2009; pp. 323–362.
74. Knopf, K. M.; Murphy, B. L.; MacMillan, S. N.; Baskin, J. M.; Barr, M. P.; Boros, E.; Wilson, J. J. *J. Am. Chem. Soc.* **2017**, *139*, 14302–14314.
75. Zaharevitz, D. W.; Holbeck, S. L.; Bowerman, C.; Svetlik, P. A. *J. Mol. Graphics Modell.* **2002**, *20*, 297–303.
76. Shoemaker, R. H. *Nat. Rev. Cancer* **2006**, *6*, 813–823.
77. Zuehlke, A. D.; Moses, M. A.; Neckers, L. *Phil. Trans. R. Soc. B* **2018**, *373*, 20160527.
78. Li, L.; Wang, L.; You, Q.-D.; Xu, X.-L. *J. Med. Chem.* **2020**, *63*, 1798–1822.
79. Capper, M. S.; Garcia, A. E.; Macia, N.; Lai, B.; Lin, J.-B.; Nomura, M.; Alihosseinzadeh, A.; Ponnurangam, S.; Heyne, B.; Shemanko, C. S.; Jalilehvand, F. *J. Biol. Inorg. Chem.* **2020**, *25*, 759–776.
80. Capper, M. S.; Garcia, A. E.; Lai, B.; Wang, B. O.; Gelfand, B. S.; Shemanko, C. S.; Jalilehvand, F. *Dalton Trans.* **2021**, *50*, 5968–5977.
81. Karges, J.; Kalaj, M.; Gembicky, M.; Cohen, S. M. *Angew. Chem. Int. Ed.* **2021**, *60*, 10716–10723.

82. Konkankit, C. C.; King, A. P.; Knopf, K. M.; Southard, T. L.; Wilson, J. J. *ACS Med. Chem. Lett.* **2019**, *10*, 822–827.
83. Herrick, R. S.; Wrona, I.; McMicken, N.; Jones, G.; Ziegler, C. J.; Shaw, J. *J. Organomet. Chem.* **2004**, *689*, 4848–4855.
84. Costa, R.; Chanawanno, K.; Engle, J. T.; Baroody, B.; Herrick, R. S.; Ziegler, C. J. *J. Organomet. Chem.* **2013**, *734*, 25–31.
85. Chanawanno, K.; Kondeti, V.; Caporoso, J.; Paruchuri, S.; Leeper, T. C.; Herrick, R. S.; Ziegler, C. J. *Dalton Trans.* **2016**, *45*, 4729–4735.
86. Schrage, B. R.; Frisinger, B. R.; Schmidtke Sobeck, S. J.; Ziegler, C. *J. Dalton Trans.* **2021**, *50*, 1069–1075.
87. Parveen, S. *Appl. Organomet. Chem.* **2020**, *34*, e5687.
88. Chow, M. J.; Licona, C.; Wong, D. Y. Q.; Pastorin, G.; Gaiddon, C.; Ang, W. H. *J. Med. Chem.* **2014**, *57*, 6043–6059.
89. Chow, M. J.; Alfiean, M.; Pastorin, G.; Gaiddon, C.; Ang, W. H. *Chem. Sci.* **2017**, *8*, 3641–3649.
90. Chow, M. J.; Licona, C.; Pastorin, G.; Mellitzer, G.; Ang, W. H.; Gaiddon, C. *Chem. Sci.* **2016**, *7*, 4117–4124.
91. Chow, M. J.; Babak, M. V.; Wong, D. Y. Q.; Pastorin, G.; Gaiddon, C.; Ang, W. H. *Mol. Pharmaceutics* **2016**, *13*, 2543–2554.
92. Chow, M. J.; Babak, M. V.; Tan, K. W.; Cheong, M. C.; Pastorin, G.; Gaiddon, C.; Ang, W. H. *Mol. Pharmaceutics* **2018**, *15*, 3020–3031.
93. Konkankit, C. C.; Vaughn, B. A.; MacMillan, S. N.; Boros, E.; Wilson, J. *J. Inorg. Chem.* **2019**, *58*, 3895–3909.
94. Ammar, A. A.; Raveendran, R.; Gibson, D.; Nassar, T.; Benita, S. *J. Med. Chem.* **2016**, *59*, 9035–9046.
95. Zanellato, I.; Bonarrigo, I.; Colangelo, D.; Gabano, E.; Ravera, M.; Alessio, M.; Osella, D. *J. Inorg. Biochem.* **2014**, *140*, 219–227.
96. Johnstone, T. C.; Lippard, S. *J. Inorg. Chem.* **2013**, *52*, 9915–9920.
97. Zheng, Y.-R.; Suntharalingam, K.; Johnstone, T. C.; Yoo, H.; Lin, W.; Brooks, J. G.; Lippard, S. J. *J. Am. Chem. Soc.* **2014**, *136*, 8790–8798.
98. Awuah, S. G.; Zheng, Y.-R.; Bruno, P. M.; Hemann, M. T.; Lippard, S. J. *J. Am. Chem. Soc.* **2015**, *137*, 14854–14857.
99. Clède, S.; Lambert, F.; Saint-Fort, R.; Plamont, M.-A.; Bertrand, H.; Vessières, A.; Policar, C. *Chem. A Eur. J.* **2014**, *20*, 8714–8722.
100. Hallett, A. J.; Placet, E.; Prieux, R.; McCafferty, D.; Platts, J. A.; Lloyd, D.; Isaacs, M.; Hayes, A. J.; Coles, S. J.; Pitak, M. B.; Marchant, S.; Marriott, S. N.; Allemann, R. K.; Dervisi, A.; Fallis, I. A. *Dalton Trans.* **2018**, *47*, 14241–14253.
101. Konkankit, C. C.; Vaughn, B. A.; Huang, Z.; Boros, E.; Wilson, J. J. *Dalton Trans.* **2020**, *49*, 16062–16066.
102. Ballesta, A.; Billy, F.; Coverdale, J. P. C.; Song, J.-I.; Sanchez-Cano, C.; Romero-Canelón, I.; Sadler, P. J. *Metallomics* **2019**, *11*, 1648–1656.
103. Clède, S.; Sandt, C.; Dumas, P.; Policar, C. *Appl. Spectrosc.* **2020**, *74*, 63–71.
104. Kronauge, J. F.; Mindiola, D. J. *Organometallics* **2016**, *35*, 3432–3435.
105. Sacksteder, L.; Lee, M.; Demas, J. N.; DeGraff, B. A. *J. Am. Chem. Soc.* **1993**, *115*, 8230–8238.
106. Favale, J. M., Jr.; Danilov, E. O.; Yarnell, J. E.; Castellano, F. N. *Inorg. Chem.* **2019**, *58*, 8750–8762.
107. King, A. P.; Marker, S. C.; Swanda, R. V.; Woods, J. J.; Qian, S.-B.; Wilson, J. J. *Chem. A Eur. J.* **2019**, *25*, 9206–9210.
108. Konkankit, C. C.; Lovett, J.; Harris, H. H.; Wilson, J. J. *Chem. Commun.* **2020**, *56*, 6515–6518.

109. Wedding, J. L.; Harris, H. H.; Bader, C. A.; Plush, S. E.; Mak, R.; Massi, M.; Brooks, D. A.; Lai, B.; Vogt, S.; Werrett, M. V.; Simpson, P. V.; Skelton, B. W.; Stagni, S. *Metallomics* **2017**, *9*, 382–390.
110. Morrison, C. N.; Prosser, K. E.; Stokes, R. W.; Cordes, A.; Metzler-Nolte, N.; Cohen, S. M. *Chem. Sci.* **2020**, *11*, 1216–1225.
111. Senft, D.; Ronai, Z. A. *Trends Biochem. Sci.* **2015**, *40*, 141–148.
112. Wek, R. C.; Cavener, D. R. *Antioxid. Redox Signal.* **2007**, *9*, 2357–2371.
113. Almanza, A.; Carlesso, A.; Chintha, C.; Creedican, S.; Doultsinos, D.; Leuzzi, B.; Luís, A.; McCarthy, N.; Montibeller, L.; More, S.; Papaioannou, A.; Püschel, F.; Sassano, M. L.; Skoko, J.; Agostinis, P.; de Belleroche, J.; Eriksson, L. A.; Fulda, S.; Gorman, A. M.; Healy, S.; Kozlov, A.; Muñoz-Pinedo, C.; Rehm, M.; Chevet, E.; Samali, A. *FEBS J.* **2019**, *286*, 241–278.
114. Ohmichi, M.; Hayakawa, J.; Tasaka, K.; Kurachi, H.; Murata, Y. *Trends Pharmacol. Sci.* **2005**, *26*, 113–116.
115. Wacker, S. A.; Houghtaling, B. R.; Elemento, O.; Kapoor, T. M. *Nat. Chem. Biol.* **2012**, *8*, 235–237.
116. Kapoor, T. M.; Miller, R. M. *Trends Pharmacol. Sci.* **2017**, *38*, 1100–1109.
117. Marker, S. C.; King, A. P.; Swanda, R. V.; Vaughn, B.; Boros, E.; Qian, S.-B.; Wilson, J. J. *Angew. Chem. Int. Ed.* **2020**, *59*, 13391–13400.
118. Mechetner, E.; Kyshtoobayeva, A.; Zonis, S.; Kim, H.; Stroup, R.; Garcia, R.; Parker, R. J.; Fruehauf, J. P. *Clin. Cancer Res.* **1998**, *4*, 389–398.
119. Ling, V. *Cancer Chemother. Pharmacol.* **1997**, *40*, S3–S8.
120. Piwnica-Worms, D.; Chiu, M. L.; Budding, M.; Kronauge, J. F.; Kramer, R. A.; Croop, J. M. *Cancer Res.* **1993**, *53*, 977–984.
121. Hsu, H.-H.; Chen, M.-C.; Baskaran, R.; Lin, Y.-M.; Day, C. H.; Lin, Y. J.; Tu, C.-C.; Padma, V. V.; Kuo, W.-W.; Huang, C.-Y. *J. Cell. Physiol.* **2018**, *233*, 5458–5467.
122. Landini, I.; Lapucci, A.; Pratesi, A.; Massai, L.; Napoli, C.; Perrone, G.; Pinzani, P.; Messori, L.; Mini, E.; Nobili, S. *Oncotarget* **2017**, *8*, 96062–96078.
123. Heffeter, P.; Pongratz, M.; Steiner, E.; Chiba, P.; Jakupec, M. A.; Elbling, L.; Marian, B.; Körner, W.; Sevelda, F.; Micksche, M.; Keppler, B. K.; Berger, W. *J. Pharmacol. Exp. Ther.* **2005**, *312*, 281–289.
124. Licona, C.; Delhorme, J.-B.; Riegel, G.; Vidimar, V.; Cerón-Camacho, R.; Boff, B.; Venkatasamy, A.; Tomasetto, C.; da Silva Figueiredo Celestino Gomes, P.; Rognan, D.; Freund, J.-N.; Le Lagadec, R.; Pfeffer, M.; Gross, I.; Mellitzer, G.; Gaiddon, C. *Inorg. Chem. Front.* **2020**, *7*, 678–688.
125. Marker, S. C.; King, A. P.; Granja, S.; Vaughn, B.; Woods, J. J.; Boros, E.; Wilson, J. *J. Inorg. Chem.* **2020**, *59*, 10285–10303.
126. Suntharalingam, K.; Johnstone, T. C.; Bruno, P. M.; Lin, W.; Hemann, M. T.; Lippard, S. J. *J. Am. Chem. Soc.* **2013**, *135*, 14060–14063.
127. Ye, R.-R.; Tan, C.-P.; Chen, M.-H.; Hao, L.; Ji, L.-N.; Mao, Z.-W. *Chem. A Eur. J.* **2016**, *22*, 7800–7809.
128. Li, C.; Ip, K.-W.; Man, W.-L.; Song, D.; He, M.-L.; Yiu, S.-M.; Lau, T.-C.; Zhu, G. *Chem. Sci.* **2017**, *8*, 6865–6870.
129. Collery, P.; Mohsen, A.; Kermagoret, A.; Corre, S.; Bastian, G.; Tomas, A.; Wei, M.; Santoni, F.; Guerra, N.; Desmaële, D.; d'Angelo, J. *Invest. New Drugs* **2015**, *33*, 848–860.
130. Wang, F.-X.; Liang, J.-H.; Zhang, H.; Wang, Z.-H.; Wan, Q.; Tan, C.-P.; Ji, L.-N.; Mao, Z.-W. *ACS Appl. Mater. Interfaces* **2019**, *11*, 13123–13133.
131. He, L.; Pan, Z.-Y.; Qin, W.-W.; Li, Y.; Tan, C.-P.; Mao, Z.-W. *Dalton Trans.* **2019**, *48*, 4398–4404.
132. Capper, M. S.; Packman, H.; Rehkämper, M. *ChemBioChem* **2020**, *21*, 2111–2115.

133. Domenichini, A.; Casari, I.; Simpson, P. V.; Desai, N. M.; Chen, L.; Dustin, C.; Edmands, J. S.; van der Vliet, A.; Mohammadi, M.; Massi, M.; Falasca, M. *J. Exp. Clin. Cancer Res.* **2020**, *39*, 276.
134. Collery, P.; Lagadec, P.; Krossa, I.; Cohen, C.; Antomarchi, J.; Varlet, D.; Lucio, M.; Guigonis, J.-M.; Scimeca, J.-C.; Schmid-Antomarchi, H.; Schmid-Alliana, A. *Trace Elem. Med. Biol.* **2022**, *71*, 126931.
135. King, A. P.; Wilson, J. J. *Chem. Soc. Rev.* **2020**, *49*, 8113–8136.
136. Ortega, E.; Vigueras, G.; Ballester, F. J.; Ruiz, J. *Coord. Chem. Rev.* **2021**, *446*, 214129.
137. Guan, R.; Xie, L.; Ji, L.; Chao, H. *Eur. J. Inorg. Chem.* **2020**, 3978–3986.
138. Leonidova, A.; Pierroz, V.; Rubbiani, R.; Heier, J.; Ferrari, S.; Gasser, G. *Dalton Trans.* **2014**, *43*, 4287–4294.
139. Leonidova, A.; Pierroz, V.; Adams, L. A.; Barlow, N.; Ferrari, S.; Graham, B.; Gasser, G. *ACS Med. Chem. Lett.* **2014**, *5*, 809–814.
140. Kastl, A.; Dieckmann, S.; Wähler, K.; Völker, T.; Kastl, L.; Merkel, A. L.; Vultur, A.; Shannan, B.; Harms, K.; Ocker, M.; Parak, W. J.; Herlyn, M.; Meggers, E. *ChemMedChem* **2013**, *8*, 924–927.
141. Mion, G.; Gianferrara, T.; Bergamo, A.; Gasser, G.; Pierroz, V.; Rubbiani, R.; Vilar, R.; Leczkowska, A.; Alessio, E. *ChemMedChem* **2015**, *10*, 1901–1914.
142. Wähler, K.; Ludewig, A.; Szabo, P.; Harms, K.; Meggers, E. *Eur. J. Inorg. Chem.* **2014**, 807–811.
143. Knoll, J. D.; Turro, C. *Coord. Chem. Rev.* **2015**, *282–283*, 110–126.
144. Bonnet, S. *Dalton Trans.* **2018**, *47*, 10330–10343.
145. Chen, Y.; Bai, L.; Zhang, P.; Zhao, H.; Zhou, Q. *Molecules* **2021**, *26*, 5679.
146. Koike, K.; Tanabe, J.; Toyama, S.; Tsubaki, H.; Sakamoto, K.; Westwell, J. R.; Johnson, F. P. A.; Hori, H.; Saitoh, H.; Ishitani, O. *Inorg. Chem.* **2000**, *39*, 2777–2783.
147. Koike, K.; Okoshi, N.; Hori, H.; Takeuchi, K.; Ishitani, O.; Tsubaki, H.; Clark, I. P.; George, M. W.; Johnson, F. P. A.; Turner, J. J. *J. Am. Chem. Soc.* **2002**, *124*, 11448–11455.
148. Pierri, A. E.; Pallaoro, A.; Wu, G.; Ford, P. C. *J. Am. Chem. Soc.* **2012**, *134*, 18197–18200.
149. Chakraborty, I.; Jimenez, J.; Sameera, W. M. C.; Kato, M.; Mascharak, P. K. *Inorg. Chem.* **2017**, *56*, 2863–2873.
150. Chakraborty, I.; Carrington, S. J.; Roseman, G.; Mascharak, P. K. *Inorg. Chem.* **2017**, *56*, 1534–1545.
151. Marker, S. C.; MacMillan, S. N.; Zipfel, W. R.; Li, Z.; Ford, P. C.; Wilson, J. *J. Inorg. Chem.* **2018**, *57*, 1311–1331.
152. Katti, K. V.; Gali, H.; Smith, C. J.; Berning, D. E. *Acc. Chem. Res.* **1999**, *32*, 9–17.
153. Darensbourg, D. J.; Ortiz, C. G.; Kamplain, J. W. *Organometallics* **2004**, *23*, 1747–1754.
154. Phillips, A. D.; Gonsalvi, L.; Romerosa, A.; Vizza, F.; Peruzzini, M. *Coord. Chem. Rev.* **2004**, *248*, 955–993.
155. Álvarez, D.; Menéndez, M. I.; López, R. *Inorg. Chem.* **2022**, *61*, 439–455.
156. Kourti, M.; Jiang, W. G.; Cai, J. *Oxid. Med. Cell. Longevity* **2017**, *2017*, 9326454.
157. Huang, Z.; Wilson, J. J. *Eur. J. Inorg. Chem.* **2021**, 1312–1324.
158. Wang, Z.; Wang, N.; Cheng, S.-C.; Xu, K.; Deng, Z.; Chen, S.; Xu, Z.; Xie, K.; Tse, M.-K.; Shi, P.; Hirao, H.; Ko, C.-C.; Zhu, G. *Chem* **2019**, *5*, 3151–3165.
159. Yao, H.; Chen, S.; Deng, Z.; Tse, M.-K.; Matsuda, Y.; Zhu, G. *Inorg. Chem.* **2020**, *59*, 11823–11833.
160. Karges, J.; Yempala, T.; Tharaud, M.; Gibson, D.; Gasser, G. *Angew. Chem. Int. Ed.* **2020**, *59*, 7069–7075.
161. Huang, Z.; King, A. P.; Lovett, J.; Lai, B.; Woods, J. J.; Harris, H. H.; Wilson, J. J. *Chem. Commun.* **2021**, *57*, 11189–11192.
162. Wexselblatt, E.; Gibson, D. *J. Inorg. Biochem.* **2012**, *117*, 220–229.